TECHNISCHE
UNIVERSITÄT
WIEN
Vienna University of Technology

D I P L O M A R B E I T

Optimal Control and Climate Change: The Combination of Two Models

Ausgeführt am Institut für
Wirtschaftsmathematik
der Technischen Universität Wien

unter der Anleitung von
Ao.Univ.Prof. Dipl.-Ing. Dr.techn. Gernot Tragler

durch
Lukas Richter
Goldschlagstraße 69/6/26
1150 Wien

Wien, Oktober 2013 _____

Abstract

In this thesis we study two types of models dealing with optimal control of global warming. The first is an optimal control model of global warming, which assumes the emissions of greenhouse gases as control variable, while the temperature increase and the concentration of greenhouse gases enter as state variables. A key feature of this model is that the decay of greenhouse gases within the atmosphere depends negatively on the temperature increase. The second is a basic growth model with global warming. We first analyse a model with constant returns to scale and then reformulate the model to obtain decreasing returns to scale. In both, a social planner maximises her/his discounted utility by choosing consumption and abatement spending.

The main goal of this thesis is to investigate a model combined of the two mentioned above. For this purpose, we implement the idea of the optimal control model of global warming that the decay of greenhouse gases is related to the actual temperature increase into the growth model with decreasing returns to scale. By using the same parameter set for the new as well as for the original growth model, we show that the outcome of both models is more or less equivalent.

Zusammenfassung

In dieser Arbeit werden zwei Arten von Modellen behandelt. Einerseits wird ein optimales Kontrollmodell des Klimawandels untersucht, welches Dynamiken der Konzentration von Treibhausgasen und der Temperatur berücksichtigt. Als Kontrolle für den Entscheidungsträger steht in diesem Modell der Ausstoß von Treibhausgasen zur Verfügung. Ein wichtiger Aspekt dieses Modells ist, dass die natürliche Rate, mit der sich der Anteil der Gase in der Atmosphäre verringert, negativ vom Temperaturanstieg abhängt. Andererseits wird ein einfaches Wachstumsmodell betrachtet, welches globale Erwärmung berücksichtigt. Zuerst wird ein Modell mit konstanten Skalenerträgen vorgestellt, welches dann aber in ein Modell mit fallenden Skalenerträgen umformuliert wird. In beiden Fällen maximiert ein sozialer Planer den diskontierten Nutzen aus dem Konsum der Individuen, und er wählt den optimalen Pfad bestehend aus dem Konsum und den Kosten, welche durch Emissionsverminderungen entstehen.

Das primäre Ziel dieser Arbeit besteht darin, ein Modell zu formulieren und zu untersuchen, welches die Eigenschaften beider oben genannten Modelle vereint. Dazu wird die Idee des Ersten, nämlich dass die Abbaurate der Treibhausgase negativ von der Temperatur abhängt, in das Wachstumsmodell mit fallenden Skalenerträgen implementiert. Im Zuge der Analyse wird festgestellt, dass bei gleich gewählten Parameterwerten kaum Unterschiede zwischen dem neuen und dem ursprünglichen Wachstumsmodell festzustellen sind.

Acknowledgements

Special thanks to my family, particularly to my parents, who made it possible for me to study and who supported me whenever it was necessary. This work would not exist without their help and patience.

I also want to thank my supervisor Prof. Dr. Gernot Tragler for his support and for sharing his experiences with me. Further, I thank Prof. Dr. Alexia Fürnkranz-Prskawetz for proposing the subject of this thesis and for her inputs. Thanks also to Dr. Dieter Grass, who helped me solving problems concerning his `Matlab` toolbox `OCMat`.

Finally, I thank my good friend Siegfried Langer for proof-reading this thesis.

Contents

Chapter 1

Introduction

Although the global warming seems to pause at the moment (for the years $1998-2012$ the temperature increase was only $0.05\,^{\circ}\mathrm{C}$ and hence smaller than the rate calculated, which is $0.12\,^{\circ}\mathrm{C}$), it seems certain that the change of our climate system is closely related to mankind. Also, within the last decades, the earth suffered many extreme weather events (hurricanes, floods, tsunamis, etc.), primarily in the Northern Hemisphere. Of course, changes of the climate system are also a result of internal variability and they are affected by external factors, which can also be natural and not only anthropogenic. However, it is very likely that the climate changes of the last 50 years were caused primarily by human activities. *"Human influence on the climate system is clear. This is evident from the increasing greenhouse gas concentrations in the atmosphere, positive radiative forcing, observed warming, and understanding of the climate system."* This is one of the conclusions of the Fifth Assessment Report by the International Panel on Climate Change (IPCC) [1]. Anthropogenic emissions of greenhouse gases (GHGs), for example carbon dioxide (CO_2) or methane (CH_4), have an impact on the average global surface temperature of our planet. The 1990s were very likely ($90-99\%$) the warmest decade since 1861, according to the IPCC.

Hence, not only extreme weather effects are problems we have to deal with. Also economies are affected, due to problems in agricultural production. If the surface temperature increases, costs due to non-optimality within the agricultural sector will occur, because farming is optimised for the current climate. The extreme weather effects, as mentioned above, often cause bad harvest, too, which is another economic problem. The IPCC 2007 [2] suggests an estimate for social costs of \$12 per ton of emitted carbon. With the level of emissions in the same year, which was 8.365 billion tons[1], the expected social costs in 2007 were about \$100 billion.

[1] http://cdiac.ornl.gov/trends/emis/tre_glob.html (last accessed on 25 October 2013)

Therefore, the change of our climate systems, the results thereof, and the possible countermeasures not only are important topics among politicians and scientists, but they are also of public interest. Hence, lots of papers exist which deal with the problems mentioned above. The overall goal of this thesis is different. Primarily, we do not want to derive optimal abatement strategies or policies concerning emissions. We want to study the impact of a change regarding an economic growth model with global warming and its outcome, if we modify one of the state dynamics to satisfy the assumption that greenhouse gases stay longer within the atmosphere if the average surface temperature increases. Thus, we start with the economic growth model by Greiner et al. [3],[4] and combine it with the model of Erickson [5].

The thesis is organised as follows. In Chapter 2, an optimal control model incorporating global warming is presented and analysed. The model contains two state variables representing anthropogenic concentration of greenhouse gases within the atmosphere and the temperature increase over pre-industrial level. The single control variable stands for emissions of GHGs. The model is analysed and solved by using Pontryagin's Maximum Principle. Deeper analysis regarding the implemented parameters is done by using bifurcation analysis and comparative statics. Moreover, a numerical example is presented. Also an analysis of a special case of the model is presented, where the emissions are exogenously given.

Chapter 3 begins with the presentation of a so-called *energy balance model* (EBM), describing the influence of changes of the average surface temperature and GHG emissions on our earth. The first version of the underlying economy is modelled such that it implies a growth model with constant returns to scale, regarding capital. After integrating the EBM into the growth model, we obtain an optimal control model with two control and three state variables. It is solved again by using the Maximum Principle. After a numerical example, the economy is modified to offer decreasing returns to scale. Furthermore, the modified model is analysed and supplemented with another numerical example. Moreover, results which are numerically computed by the use of the `Matlab` toolbox `OCMat` are presented. The chapter ends with the comparative statics for the modified model.

Next, the two models of the previous chapters are combined and presented in Chapter 4. The obtained system is solved and analysed with the same tools as the models before. After another numerical example, the comparative statics concerning the newly implemented parameter is given.

Finally, in Chapter 5 a conclusion closes the thesis. A short summary of all results is given and the outcome and final statements are discussed. Some of the technical details of the analysis is deferred to the Appendix.

Chapter 2

The Erickson Model

In what follows we study a model presented by Erickson [5]. It describes a trade-off between benefits as well as costs due to anthropogenic GHG emissions and consequential global warming. Erickson uses the GHG concentration stock rather than the flow in the stated dynamics.

2.1 The Model

We consider the following two-state, one-control model in continuous time. The state equations are given by

$$\dot{G}(t) = m(t) - \beta\, G(t) + \gamma\, G(t)\, T(t) = m(t) - [\beta - \gamma\, T(t)]G(t), \tag{2.1}$$

$$\dot{T}(t) = \delta(\varepsilon\, G(t) - T(t)), \tag{2.2}$$

$$G(0) = G_0 \geq 0, T(0) = T_0 \geq 0,$$

$$\beta, \gamma, \delta, \varepsilon \geq 0,$$

where $G(t)$ describes the atmospheric concentration of anthropogenic GHG in billions of tons of CO_2 equivalent and $T(t)$ the global temperature in degrees Celsius, both at time t. Here, $T = 0$ means that the temperature is at pre-industrial level. Also measured in billions of tons of CO_2 equivalent, $m(t)$, is the control variable denoting the rate of anthropogenic GHG emissions. In (2.1), the GHG concentration increases by emissions and decreases by the environmental absorption rate $\beta - \gamma T(t)$, which negatively depends on the temperature $T(t)$. This relation is implemented to be consistent with the circumstances that the absorption rate decreases with higher surface temperature. We should mention here that this formulation also allows the atmosphere to become a carbon source (if $\beta - \gamma\, T(t) < 0$). The temperature positively depends on the difference between the equilibrium temperature increase $\varepsilon\, G(t)$ and the current temperature $T(t)$ multiplied by

a constant δ. Last, we define the social planner's infinite-horizon objective function given by

$$\max_{m(t)} \int_0^\infty e^{-rt}(a \ln m(t) - b\, T(t))\, dt, \tag{2.3}$$
$$a, b > 0.$$

She/He maximises benefits due to emissions, but also takes into account disadvantages of a raising surface temperature, which are a consequence of too much emissions. In (2.3), $r > 0$ denotes the discount rate, describing how the planner values the future utility. The social utility function is modelled to be increasing and concave in $m(t)$ and linearly declining in $T(t)$.

Note that from now on the time argument t will often be omitted for the sake of convenience.

2.2 The Uncontrolled Erickson Model

Before we start with the analysis of the model presented in the previous section, we study the dynamics of the uncontrolled version of the model. Therefore, the following system of autonomous ordinary differential equations is given

$$\begin{aligned}
&\dot{G} = m - (\beta - \gamma\, T)G,\\
&\dot{T} = \delta(\varepsilon\, G - T),\\
&G(0) = G_0 \geq 0, T(0) = T_0 \geq 0,\\
&m, \beta, \gamma, \delta, \varepsilon \geq 0.
\end{aligned}$$

In contrast to the model of Section 2.1, we consider an exogenous GHG emission m and assume that it is non negative. To derive steady states we set $\dot{G} = \dot{T} = 0$ and compute solutions of the obtained system.

Proposition 2.1. *Depending on m, one of the following statements is true.*

1. *If $m < \frac{\beta^2}{4\,\gamma\,\varepsilon}$ holds, the problem yields two steady states, which are given by*

$$\begin{aligned}
G^*_{1,2} &= \frac{\beta}{2\,\gamma\,\varepsilon} \pm \sqrt{\frac{\beta^2}{4\,\gamma^2\,\varepsilon^2} - \frac{m}{\gamma\,\varepsilon}},\\
T^*_{1,2} &= \frac{\beta}{2\,\gamma} \pm \sqrt{\frac{\beta^2}{4\,\gamma^2} - \frac{m\,\varepsilon}{\gamma}}.
\end{aligned}$$

2. *If* $m = \frac{\beta^2}{4\,\gamma\,\varepsilon}$*, the problem yields one steady state, which is given by* $G^* = \frac{\beta}{2\,\gamma\,\varepsilon}$ *respectively* $T^* = \frac{\beta}{2\,\gamma}$*.*

3. *If* $m > \frac{\beta^2}{4\,\gamma\,\varepsilon}$ *holds, the problem has no steady states.*

Proof. See Appendix A.1. ■

2.2.1 Stability

Based on the results of Proposition 2.1, we now analyse the stability of the steady states.

We start with the case of Proposition 2.1.1: The Jacobian for the higher steady state is given by

$$J_1(G_1^*, T_1^*) = \begin{pmatrix} -\beta + \frac{1}{2}\left(\beta + \sqrt{\beta^2 - 4\,\gamma\,\varepsilon\,m}\right) & \frac{1}{2\,\varepsilon}\left(\beta + \sqrt{\beta^2 - 4\,\gamma\,\varepsilon\,m}\right) \\ \delta\,\varepsilon & -\delta \end{pmatrix}.$$

We substitute $x := \beta + \sqrt{\beta^2 - 4\,\gamma\,\varepsilon\,m}$ and compute the eigenvalues of J_1. Then, we get

$$\lambda_{1,2} = \underbrace{\frac{-\beta + \frac{1}{2}\,x - \delta}{2}}_{=:A} \pm \sqrt{\left(\frac{-\beta + \frac{1}{2}\,x - \delta}{2}\right)^2 - (\beta\,\delta - \delta\,x)}. \tag{2.5}$$

Note that with the assumption $0 \leq m < \frac{\beta^2}{4\,\gamma\,\varepsilon}$, the condition $\beta < x \leq 2\,\beta$ holds. As a consequence, we get that $\beta\,\delta - \delta\,x < 0$ holds and therefore the expression under the root is strictly positive. Furthermore, $\sqrt{\left(\frac{-\beta+\frac{1}{2}\,x-\delta}{2}\right)^2 - (\beta\,\delta - \delta\,x)} > |A|$ and $0 > -\frac{\delta}{2} \geq A > -\frac{\delta}{2} - \frac{\beta}{4}$ are true. Hence, we get one positive and one negative eigenvalue, which means that the steady state is an unstable saddle-node.

With the substitution $y := \beta - \sqrt{\beta^2 - 4\,\gamma\,\varepsilon\,m}$ ($0 \leq y < \beta$ holds for the current assumptions) the Jacobian of the lower steady state can be written as

$$J_2(G_2^*, T_2^*) = \begin{pmatrix} -\beta + \frac{1}{2}\,y & \frac{1}{2\,\varepsilon}\,y \\ \delta\,\varepsilon & -\delta \end{pmatrix}.$$

The eigenvalues are as in equation (2.5), if we replace x by y. Note, because of $\beta\,\delta - \delta\,y > 0$, the expression

$$\sqrt{\left(\frac{-\beta + \frac{1}{2}\,y - \delta}{2}\right)^2 - (\beta\,\delta - \delta\,y)} < \left|\frac{-\beta + \frac{1}{2}\,y - \delta}{2}\right| \tag{2.6}$$

holds, if the radicand is non negative. Furthermore, the condition $0 > -\frac{\delta}{2} - \frac{\beta}{4} > \frac{-\beta+\frac{1}{2}\,y-\delta}{2} \geq -\frac{\delta}{2} - \frac{\beta}{2}$ is true, so it is guaranteed, that the real parts of the eigenvalues

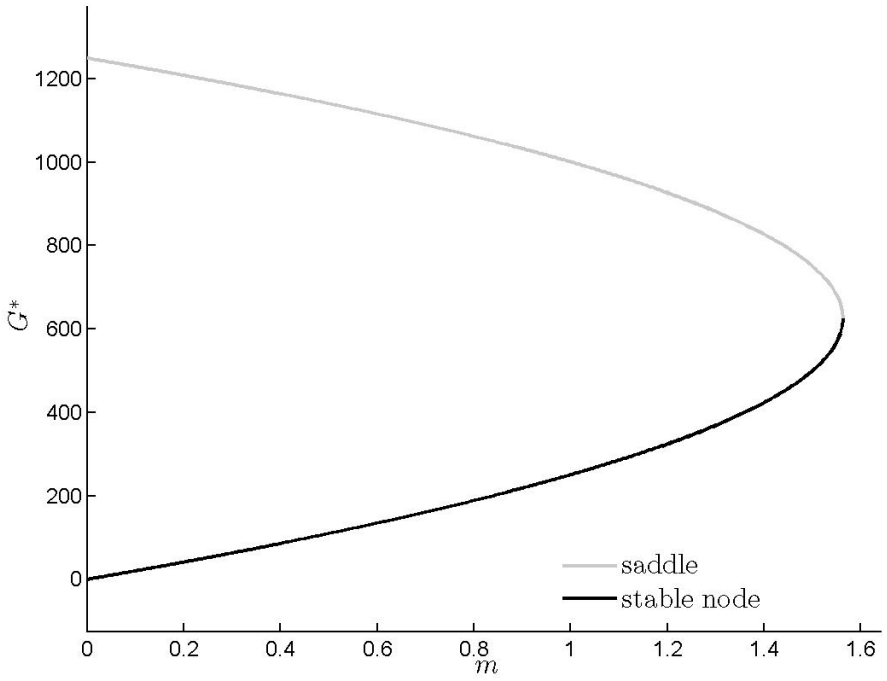

Figure 2.1: Bifurcation diagram for the uncontrolled Erickson model with parameter values $\beta = 0.005$, $\gamma = 0.001$, $\delta = 0.02$ and $\varepsilon = 0.004$.

are negative and therefore the steady state is stable. Depending on the sign of the radicand on the lefthand side in (2.6), the steady state is either a node or a focus.

In the case of the existence of only one steady state (Proposition 2.1.2), the corresponding Jacobian is

$$J(G^*, T^*) = \begin{pmatrix} -\frac{\beta}{2} & \frac{\beta}{2\varepsilon} \\ \delta\,\varepsilon & -\delta \end{pmatrix}.$$

The eigenvalues are $\lambda_1 = 0$ and $\lambda_2 = -\frac{\beta}{2} - \delta < 0$. It is not obviously clear whether the equilibrium is stable or not. We leave this case open for deeper discussion because the stability thereof is not directly evident. Keep in mind that this scenario occurs with probability zero, because there is only one value of m for this case to hold.

In Figure 2.1 we see the bifurcation diagram for parameter values $\beta = 0.005$, $\gamma = 0.001$, $\delta = 0.02$ and $\varepsilon = 0.004$ in the (m, G)-space. We see, as shown in Proposition 2.1, that the problem yields two steady states for $0 \leq m < \frac{\beta^2}{4\gamma\varepsilon} = 1.5625$. The high steady state is an unstable saddle-node, and the low steady state is a stable node. For values of m which are greater than 1.5625 the system has no equilibrium. Note that we only show the diagram for the steady-state values of the GHG concentration and not for the

temperature as it is only a linear transformation ($T^* = \varepsilon G^*$).

2.2.2 Special Case: $m = 0$

Now we investigate a special case of the previous model and set the GHG emissions $m = 0$ (see also Figure 2.1 for $m = 0$). In that case, the model simplifies to

$$\begin{aligned}
&\dot{G} = -(\beta - \gamma T)G,\\
&\dot{T} = \delta(\varepsilon G - T),\\
&G(0) = G_0 \geq 0, T(0) = T_0 \geq 0,\\
&\beta, \gamma, \delta, \varepsilon \geq 0.
\end{aligned}$$

Corresponding to Proposition 2.1.1, the system yields two steady states, $G_1^* = \frac{\beta}{\gamma\varepsilon}$ with $T_1^* = \frac{\beta}{\gamma}$ and $G_2^* = 0$ together with $T_2^* = 0$, respectively. The Jacobians of the two equilibria are given by

$$J_1(G_1^*, T_1^*) = \begin{pmatrix} 0 & \frac{\beta}{\varepsilon} \\ \delta\varepsilon & -\delta \end{pmatrix} \text{ and } J_2(G_2^*, T_2^*) = \begin{pmatrix} -\beta & 0 \\ \delta\varepsilon & -\delta \end{pmatrix},$$

with eigenvalues $\lambda_{1,1} = -\frac{\delta}{2} + \sqrt{\left(\frac{\delta}{2}\right)^2 + \delta\beta}$ and $\lambda_{1,2} = -\frac{\delta}{2} - \sqrt{\left(\frac{\delta}{2}\right)^2 + \delta\beta}$ for J_1, and $\lambda_{2,1} = -\beta$ and $\lambda_{2,2} = -\delta$, respectively, where the first index denotes the Jacobian the eigenvalue belongs to and the second enumerates the eigenvalues. As the eigenvalues of the Jacobian which belongs to the second steady state are negative, it is a stable node. The first steady state is a saddle-point because one of the eigenvalues is positive and the other one is negative. In Figure 2.2 the dynamics of the model for the same parameter values as before are shown ($\beta = 0.005$, $\gamma = 0.001$, $\delta = 0.02$ and $\varepsilon = 0.004$). The dark curves characterise several trajectories for various initial conditions. The trajectory through the higher steady state (dash-dotted curve) is the stable manifold of the equilibrium. We observe that for all initial values to the right of this curve, the system explodes. For the ones on the left, the system converges to the stable node. It is obvious that we prefer initial values, such that the system converge to the equilibrium at the origin or to the higher one. On the other hand, we do not want dynamics where the system explodes.

2.3 Analysis of the Erickson Model

We solve the optimal control problem by applying Pontryagin's Maximum Principle (see, e.g., Feichtinger and Hartl [6]). Therefore, we formulate the current-value Hamiltonian

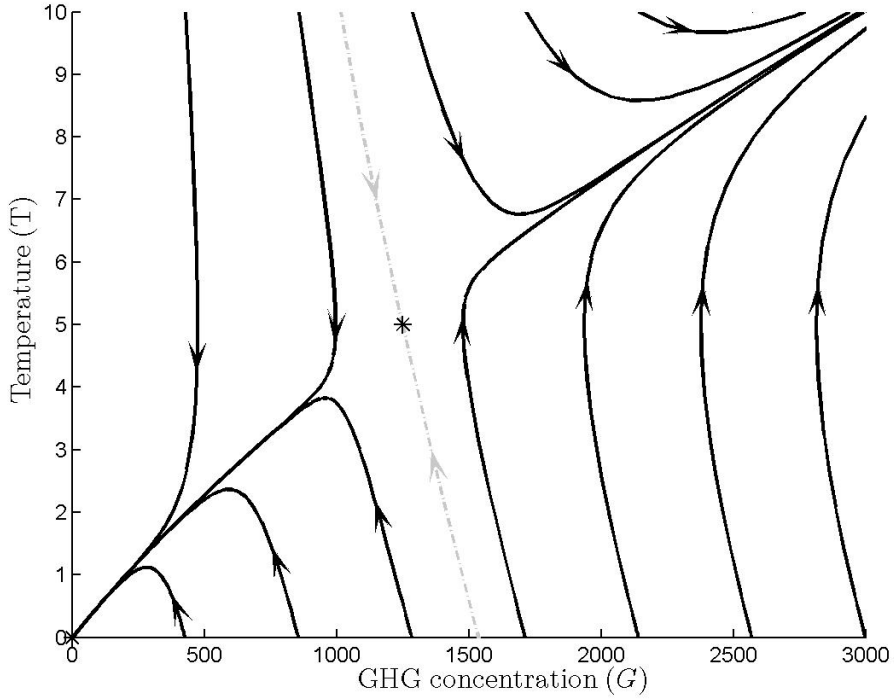

Figure 2.2: Phase portrait for the Erickson model without control. Parameter values are $m = 0$, $\beta = 0.005$, $\gamma = 0.001$, $\delta = 0.02$ and $\varepsilon = 0.004$.

given by

$$H = a \ln m - bT + \mu_1(m - \beta G + \gamma GT) + \mu_2(\delta(\varepsilon G - T)).$$

Keep in mind that the variables m, G, T, μ_1, μ_2 all depend on time, t. Here μ_1 and μ_2 denote the co-state variables. From the first-order conditions we get

$$m = -\frac{a}{\mu_1}, \tag{2.7}$$

$$\dot{\mu}_1 = \mu_1(r + \beta - \gamma T) - \mu_2 \delta \varepsilon, \tag{2.8}$$

$$\dot{\mu}_2 = -\mu_1 \gamma G + \mu_2(r + \delta) + b, \tag{2.9}$$

together with (2.1)-(2.2). Setting the right hand sides of (2.1)-(2.2) and (2.8)-(2.9) equal to zero and using equation (2.7), we can compute the steady state solutions. For the GHG concentration we get

$$G^* = \frac{1}{2\gamma\varepsilon}\left(\frac{a\gamma(r+2\delta)}{b\delta} + \beta \pm \sqrt{\left(\beta + \frac{a\gamma(r+2\delta)}{b\delta}\right)^2 - \frac{4a\gamma(r+\beta)(r+\delta)}{b\delta}}\right). \tag{2.10}$$

Therefore, a necessary and sufficient condition for a unique steady state is given by the equation

$$\left(\beta + \frac{a\gamma(r+2\delta)}{b\delta}\right)^2 = \frac{4a\gamma(r+\beta)(r+\delta)}{b\delta}. \tag{2.11}$$

For the temperature we compute the steady-state value

$$T^* = \varepsilon G^*,$$

and for the control variable

$$m^* = \frac{a}{b\delta\varepsilon}\left((r+\beta)(r+\delta) - \gamma\varepsilon(r+2\delta)G^*\right). \tag{2.12}$$

To specify the number of steady states we give the following Proposition.

Proposition 2.2. *If*

$$r < \frac{1}{4}\left(\sqrt{(\beta+2\delta)^2 + \frac{4b\beta^2\delta}{a\gamma}} - (\beta+2\delta)\right) \tag{2.13}$$

holds, then the problem yields two steady states.

Proof. See Appendix A.2. ■

Remark. *Proposition 2.2 is only a sufficient condition.*

An interesting issue is whether the environment is a carbon sink, which is defined as $\beta - \gamma T > 0$, in the long run.

Proposition 2.3. *Let* (2.13) *be fulfilled. Then* $r < \frac{b\beta\delta}{a\gamma} - 2\delta$ *guarantees that the lower steady state is a carbon sink.*

Proof. See Appendix A.3. ■

Remark. *The greater steady state may or may not be a carbon sink.*

Sufficient Optimality Conditions

In the following, we assume parameter values such that at least one steady state exists.

The Hessian of the Hamiltonian is given by the symmetric matrix

$$\mathcal{H}(H) = \begin{pmatrix} -\frac{a}{m^2} & 0 & 0 \\ 0 & 0 & \mu_1\gamma \\ 0 & \mu_1\gamma & 0 \end{pmatrix}.$$

As the eigenvalues are given by $\lambda_{\mathcal{H},1} = -\frac{a}{m^2}$, $\lambda_{\mathcal{H},2} = \mu_1\,\gamma$, and $\lambda_{\mathcal{H},3} = -\mu_1\,\gamma$, two are negative and one is positive. This implies that the Hessian is indefinite and we cannot guarantee that the steady state(s) of the system are actual optimal solutions.

2.4 Numerical Example

For a better illustration we give a short numerical example in this section. To be consistent with recent studies we assume $\beta = 0.005$ and $\delta = 0.02$ as in Nordhaus [7]. Cox et al. [8] say that by the end of the 21st century the environment will no longer be a carbon sink and the temperature will have increased by about 5 °C, so we set γ such that $0.005 - \gamma \cdot 5 = 0$ holds, implying $\gamma = 0.001$. The parameter ε is chosen to be consistent with Nordhaus [7] and Pachauri and Reisinger [2] who give the best estimate for a temperature increase by 3 °C if the GHG concentration is doubled from the current value of 800 billion tons, so $\varepsilon = 0.004$. The parameters a and b are set equal to one, $a = b = 1$. The discount rate r is difficult to measure, but in this example let r be 0.001. As Proposition 2.2 and 2.3 allow r to be within the interval $(0, 0.0046)$ for the parameters we chose, we get two steady states, and the lower one will stay a carbon sink. In summary, we have the following parameter values: $a = b = 1, r = 0.001, \beta = 0.005, \gamma = 0.001, \delta = 0.02, \varepsilon = 0.004$.

The values of the state and control variables for the lower steady state are then $G_l^* = 262.5$, $T_l^* = 1.05$, and $m_l^* = 1.036875$. The higher steady state is not feasible because the emissions are negative ($G_h^* = 1500$, $T_h^* = 6$, $m_h^* = -1.5$). As eigenvalues of the Jacobian of the feasible steady state we compute $\lambda_1 = -0.0037, \lambda_2 = 0.0047, \lambda_3 = -0.021$, and $\lambda_4 = 0.022$, and therefore it is saddle-point stable.

2.5 Special Case: $\gamma = 0$

Now we study the case for which we assume that the decay of anthropogenic GHGs within the atmosphere is not affected by a change within the average surface temperature.

If we set $\gamma = 0$, the model (2.1)-(2.3) simplifies to:

$$\begin{aligned} \max_{m(t)} \quad & \int_0^\infty e^{-rt}(a \ln m(t) - bT(t))\,dt \\ \text{s.t.} \quad & \dot{G}(t) = m(t) - \beta G(t), \\ & \dot{T}(t) = \delta(\varepsilon G(t) - T(t)). \end{aligned} \tag{2.14}$$

Proposition 2.4. *The steady state of* (2.14) *is given by*

$$\begin{aligned} G^* &= \frac{a(r+\beta)(r+\delta)}{b\beta\delta\varepsilon}, \\ T^* &= \frac{a(r+\beta)(r+\delta)}{b\beta\delta}, \\ m^* &= \frac{a(r+\beta)(r+\delta)}{b\delta\varepsilon}, \end{aligned} \tag{2.15}$$

and it is unique, and saddle-point stable.

Proof. See Appendix A.4. ■

It is interesting to consider changes in the steady-state values as the parameter values change (Table 2.1). Both state variables as well as the control variable positively depend on the parameter a, which values the factor of emissions in the utility function. Further, they decrease in the parameter b, the parameter for the costs of global warming. All three steady-state values increase in the discount rate r and fall in the temperature delay factor δ. Note that an increase in δ means a faster convergence of the temperature to its equilibrium value. The absorption parameter β has positive effects on the steady state emissions and negative ones on the GHG concentration and the temperature. Last but not least, the conversion parameter ε has no impact on the optimal temperature but has negative effects on the optimal GHG concentration and the optimal emissions. For an overview of the comparative static relationships, see Table 2.1.

	a	b	r	β	δ	ε
G^*	$+$	$-$	$+$	$-$	$-$	$-$
T^*	$+$	$-$	$+$	$-$	$-$	0
m^*	$+$	$-$	$+$	$+$	$-$	$-$

Table 2.1: Comparative statics of the special model (2.14).

2.6 Further Analysis

In this section we will discuss further aspects of the model that have not been presented by Erickson [5]. Note that we now deal with the base model, (2.1)-(2.3), which in contrary to the previous section assumes $\gamma > 0$.

First we investigate the sign of the steady-state values of the control respectively the state variables. For that purpose, we assume parameter values such that two steady states exist. It is easy to see that G^* and T^* are positive for the high as well as for the low

steady state. To see this, we start with equation (2.10) and define $A := \frac{a\gamma(r+2\delta)}{b\delta} + \beta$ and $B := \frac{4a\gamma(r+\beta)(r+\delta)}{b\delta}$. Then (2.10) can be written as $G^* = \frac{1}{2\gamma\varepsilon}(A \pm \sqrt{A^2 - B})$ and therefore the sign of G^* only depends on the sign of $A \pm \sqrt{A^2 - B}$. Because we considered the existence of two steady states, which is equivalent to $A^2 > B$, $A + \sqrt{A^2 - B} > 0$ and $A - \sqrt{A^2 - B} > 0$ hold. Hence, $G^* > 0$ is true, and as the relation $T^* = \varepsilon G^*$ holds, this also implies $T^* > 0$.

It is not possible to derive similar statements for m, but we want to mention that a steady state can only be admissible if $m > 0$ holds. Technically this is true, because m enters the objective function as $\ln m$. But this requirement seems also useful for reasons of realism. A negative GHG emission would imply that mankind has a technology to degrade the GHG concentration of the atmosphere.

2.6.1 Optimal Behaviour in the Main Model

In this section we again deal with the full model (2.1)-(2.3). The parameter values are the same as in Section 2.4.

As we see in the phase portrait of the uncontrolled model (Figure 2.2), there exists an area on the right side of the stable manifold (dash-dotted arc) where the system explodes. For the main model this implies that if we start with initial values in that area, we have no chance to control the system in a way to head to the steady state (this would only be possible if we allow $m < 0$). Anyways, we do not want to discuss optimal controls for this area, as initial points are currently not realistic there. Erickson [5] considers the current GHG concentration at a level of about 800 billion tons, and according to Pachauri and Reisinger [2] the temperature increase over pre-industrial level currently is about 0.74 °C.

Phase portrait and classification of trajectories

The results respectively plots presented in what follows were computed by using the `Matlab` toolbox `OCMat`[1]. The trajectories displayed in the phase portraits and the time paths were computed by using a so-called BVP approach (see Grass [9] for a detailed description).

In Figure 2.3 we see the phase portrait in the state space. We now classify four groups of initial conditions. These are identified by the four combinations of a low/high initial GHG concentration and a low/high initial temperature. One trajectory of each group is highlighted in Figure 2.3 (dash-dotted) and we will study their behaviour regarding the control respectively the state variables in the next section.

[1] http://orcos.tuwien.ac.at/research/ocmat_software/ (last accessed on 28 October 2013)

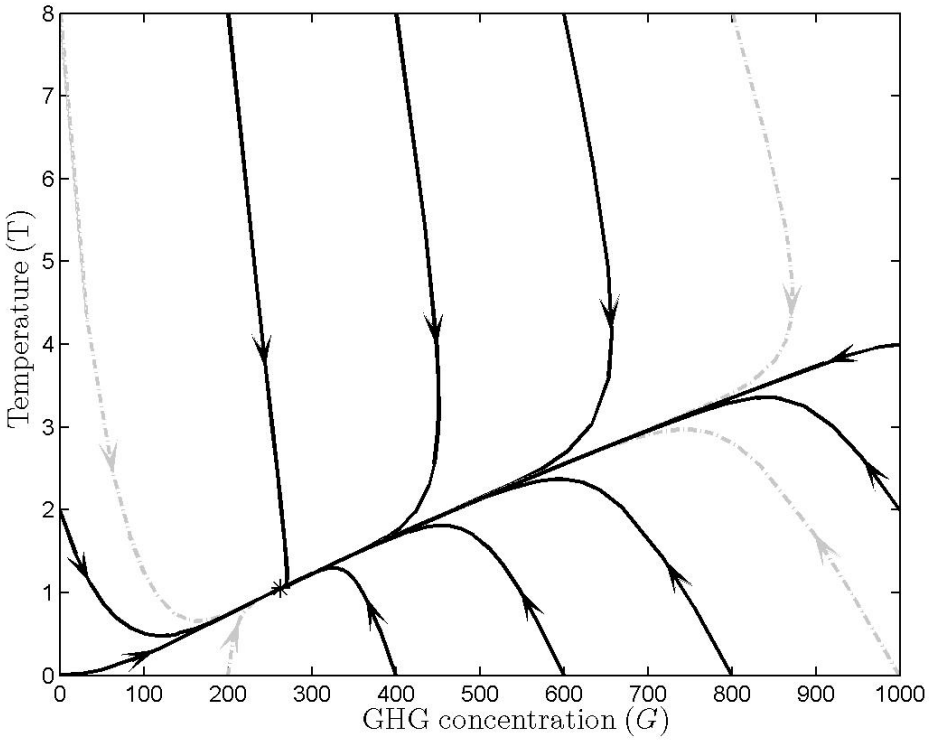

Figure 2.3: Phase portrait of the main model in the (G, T)-space.

Optimal time paths

First, we consider the case where both initial values are low ($G(0) = 200$ and $T(0) = 0$). This means, that the surface temperature is at a pre-industrial level and the GHG concentration is relatively low at 200 billion tons of CO_2 equivalent. Figure 2.4(a) shows that the optimal control is a convex and decreasing function of time. While the state variables are small, it is optimal to emit more, while we lower the emissions as we approach the steady state. The related paths of the state variables denote concave and increasing functions. As we see in Figure 2.4(b), the temperature (dash-dotted) converges faster to its steady-state value, while the GHG concentration (black) takes longer to approach its long-term level.

Another case is shown in Figure 2.5. Here we start with initial values $G(0) = 0$ and $T(0) = 8$. We see that it is optimal to start with a low emission level. Then, m should be increased to a level above the steady-state level, and later it is optimal to reduce the emissions monotonically until the long-run value is reached. On the other side, this behaviour leads to a fast decrease of the temperature to a level close to (but under) the steady-state value. Afterwards it approaches the long-term value. The G-curve is again concave and increasing and behaves like in the previous case.

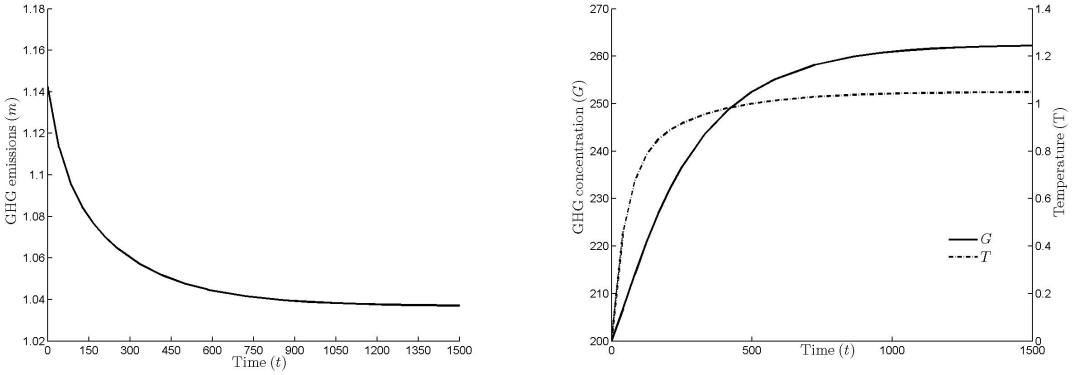

(a) (b)

Figure 2.4: Optimal time path of the control (a) and the state variables (b) for low initial values $G(0) = 200$ and $T(0) = 0$. In (b) the solid black curve denotes the GHG concentration, while the dash-dotted curve describes the temperature.

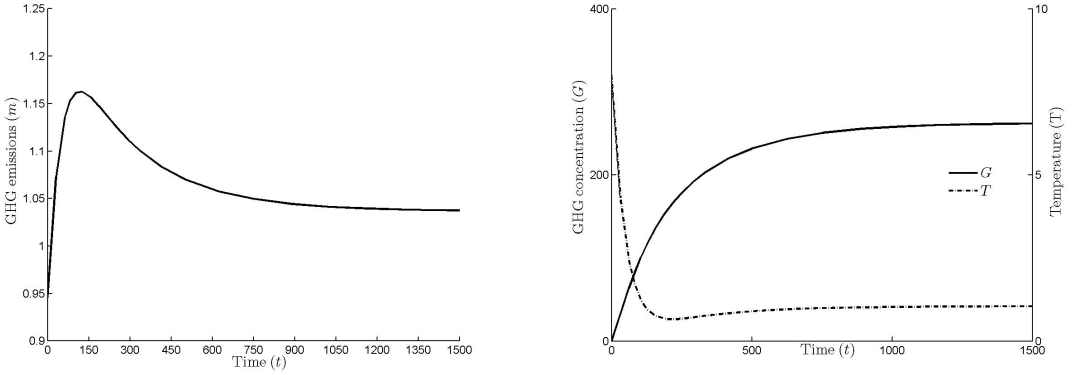

(a) (b)

Figure 2.5: Optimal time path of the control (a) and the state variables (b) for a low initial value $G(0) = 0$ and a high initial value $T(0) = 8$. In (b) again the solid black curve denotes the GHG concentration, and the dash-dotted curve describes the temperature.

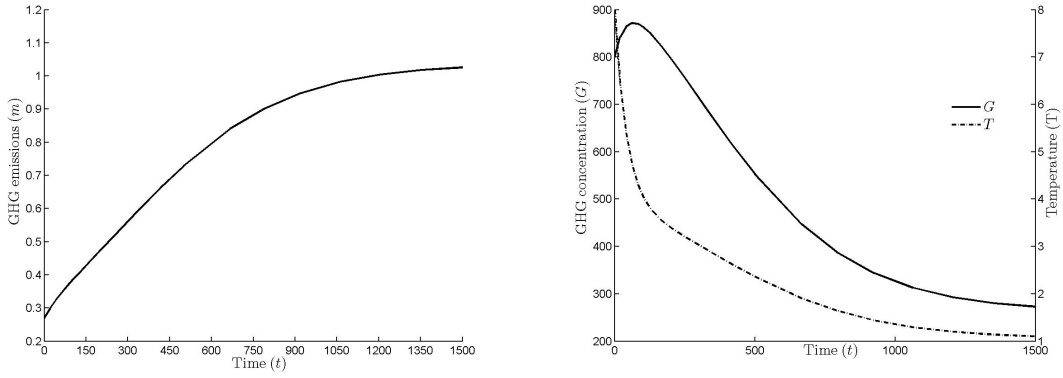

(a) (b)

Figure 2.6: Optimal time path of the control (a) and the state variables (b) for high initial values $G(0) = 800$ and $T(0) = 8$. In (b) again the GHG concentration is solid black, while the temperature is dash-dotted.

The next trajectory we investigate corresponds to high initial conditions ($G(0) = 800$ and $T(0) = 8$). We see in Figure 2.6(a) that in the beginning there are low GHG emissions, but they increase in a concave way over time. In (b), we see that the temperature is a decreasing and convex curve, while the GHG concentration even increases in the short run. In the long run, it falls to its steady-state value.

The last case we study is the one with a high initial value of GHG concentration ($G(0) = 1000$) and a low level of temperature ($T(0) = 0$). In this situation we optimally start at a low emission level, which gets even lower in the very short run. Afterwards, m should be raised in a concave way (see Figure 2.7(a)). The GHG concentration is a decreasing and convex function in this case, whereas the function of the temperature is non-monotonic. At first it explodes to reach a peak nearly three times as high as its steady-state value (Figure 2.7(b)).

2.6.2 More on the Special Model

In the following, we present further analysis and several plots for the special model presented in Section 2.5. For the parameters a, b, r, β, δ, and ε we use the same values as in Section 2.4. Note that in this model γ equals zero.

In Figure 2.8, we see the phase portrait of the problem with several trajectories. Note that the trajectories corresponding to initial values with low G and T, low G and high T, or high G and low T behave like the ones presented in the previous section. Therefore, the time paths for the state variables are similar to the ones shown in Figures 2.4(b), 2.5(b), and 2.7(b), respectively. The control, m, stays basically constant at a level of about 1.575 millions of tons of CO_2 equivalent for all initial values (the time path for

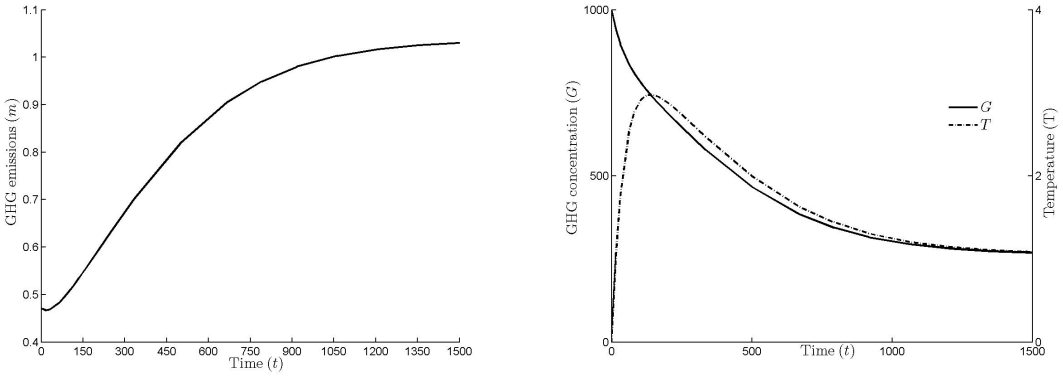

(a) (b)

Figure 2.7: Optimal time path of the control (a) and the state variables (b) for a high initial value of G, $G(0) = 1000$, and a low T, $T(0) = 0$. In (b) again the GHG concentration is solid black, and the temperature is dash-dotted.

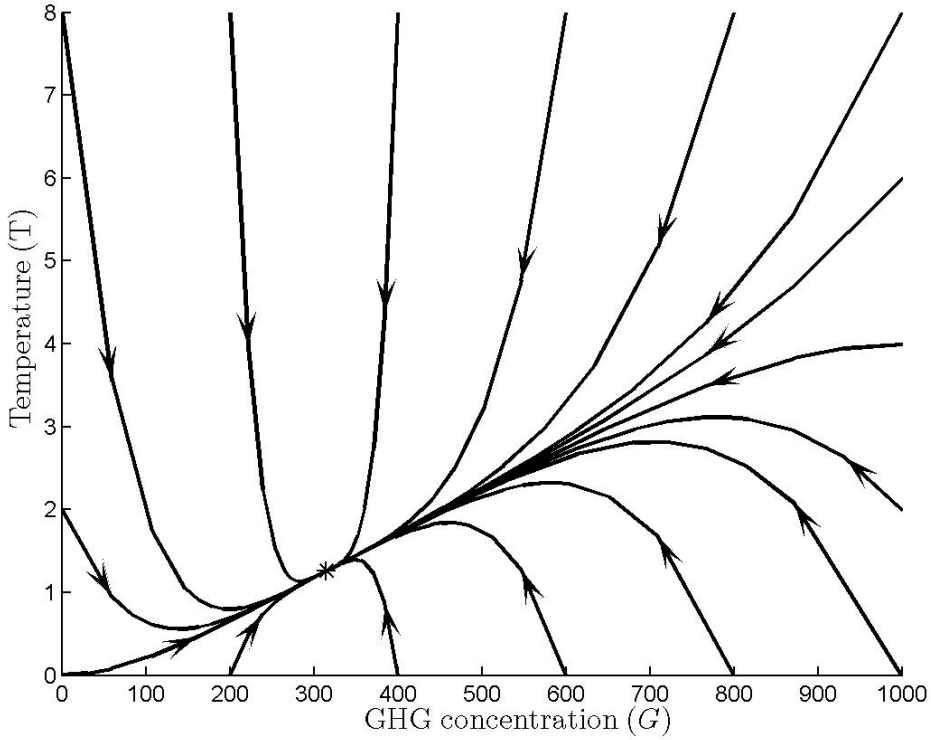

Figure 2.8: Phase portrait in the state space for the special model with $\gamma = 0$.

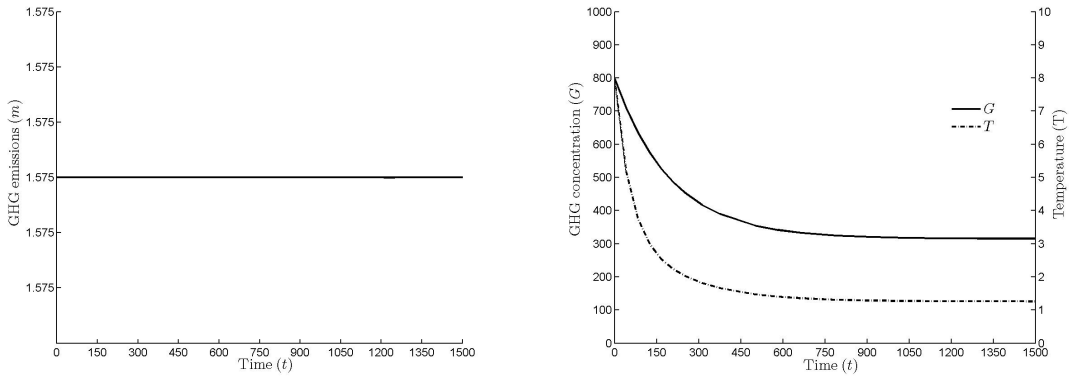

(a) (b)

Figure 2.9: Optimal time path of the control (a) and the state variables (b) for the special model with high initial values ($G(0) = 800, T(0) = 8$). In (b) the GHG concentration is the black curve, and the temperature is the dash-dotted one.

$G(0) = 800$ and $T(0) = 8$ is shown in Figure 2.9(a)).

The only case where the optimal paths of the state variables differ from the full model with $\gamma \neq 0$ is for high initial conditions for both states. An example (for $G(0) = 800$ and $T(0) = 8$) is given in Figure 2.9(b), and we see that both state variables are decreasing and convex over time.

2.6.3 Further Details on the Existence of Steady States

In Proposition 2.2 we only gave a sufficient condition for the problem to have two steady states. We now aim for conditions which are necessary and sufficient. For that purpose, we need to analyse the expression under the square root in (2.10). If this expression is positive, the problem yields two steady states, as we mentioned above. It yields one, if the expression equals zero, and it has no steady states otherwise. For a more detailed statement we give the following proposition.

Proposition 2.5. *Let a, b, r, β, γ, δ, and ε be positive. Define*

$$g(r) := \left(\beta + \frac{a\gamma(r+2\delta)}{b\delta}\right)^2 - \frac{4a\gamma(r+\beta)(r+\delta)}{b\delta}$$

and let r_1 respectively r_2 be the lower and the greater zero of g (if they exist).

1. *If $\frac{a\gamma}{b\delta} - 4 < 0$ holds, the problem (2.1)-(2.3) yields two steady states, for $r \in (0, r_2)$.*
2. *If $\frac{a\gamma}{b\delta} - 4 > 0$ holds, the problem yields two steady states*
   (a) *for every parameter value of r if*

   i. $\frac{\beta}{2} + \delta - \frac{a\gamma}{b} < 0$ *holds, or*

   ii. g *has no zeros.*

(b) *for* $r \in (0, r_1) \cup (r_2, \infty)$, *if* $\frac{\beta}{2} + \delta - \frac{a\gamma}{b} > 0$ *holds and* g *has*

   i. *one (then set* $r_1 = r_2$*), or*

   ii. *two zeros.*

3. *If* $\frac{a\gamma}{b\delta} - 4 = 0$ *and*

(a) $3\delta - \frac{\beta}{2} \geq 0$ *hold, then the problem yields two steady states for all* r.

(b) $3\delta - \frac{\beta}{2} < 0$ *hold, then the problem yields two steady states for* $r \in \left(0, \frac{\beta^2 + 64\delta^2}{8(\beta - 6\delta)}\right)$.

Proof. See Appendix A.5. ■

2.6.4 Analysis on the "Quadratic" Parameter γ

In the previous sections we carried out bifurcation analyses regarding the discount rate, r. In Section 2.5 we investigated the "easy" case ($\gamma = 0$), which means that there is no quadratic part in the problem. But as the complexity of this model comes from the quadratic part of the formulation, it will be interesting to analyse the behaviour of the system (existence of steady states, stability) depending on γ. The following proposition gives an overview of parameter conditions for the problem to yield zero, one, or two steady states.

Proposition 2.6. *Let* $a, b, r, \beta, \gamma, \delta, \varepsilon > 0$ *hold. Define*

$$k(\gamma) := \gamma^2 + \gamma \left(-\frac{2br\delta(2(r+\delta)+\beta)}{a(r+2\delta)^2} \right) + \left(\frac{b\beta\delta}{a(r+2\delta)} \right)^2, \tag{2.16}$$

and let γ_1 *and* γ_2 *denote the zeros of* k *(if they exist).*

1. *If* $r = -\frac{\delta}{2} + \sqrt{\left(\frac{\delta}{2}\right)^2 + \beta\delta}$ *holds, the problem* (2.1)-(2.3) *yields*

(a) *one steady state for* $\gamma = \frac{br\delta(2(r+\delta)+\beta)}{a(r+2\delta)^2}$.

(b) *two steady states for all other values of* γ.

2. *If* $r < -\frac{\delta}{2} + \sqrt{\left(\frac{\delta}{2}\right)^2 + \beta\delta}$ *holds, the problem yields two steady states for all values of* γ.

3. *If* $r > -\frac{\delta}{2} + \sqrt{\left(\frac{\delta}{2}\right)^2 + \beta\delta}$ *holds, the problem yields*

(a) *no steady state for* $\gamma \in (\gamma_1, \gamma_2)$.

(b) one steady state for $\gamma \in \{\gamma_1, \gamma_2\}$.

(c) two steady states for $\gamma \in (0, \gamma_1) \cup (\gamma_2, \infty)$.

Proof. See Appendix A.6. ■

Remark. *The zeros of* (2.16) *are given by:*

$$\gamma_{1,2} = \frac{b\delta}{a(r+2\delta)} \left\{ r[2(r+\delta)+\beta] \pm 2\sqrt{(r+\beta)(r+\delta)[r^2+\delta(r-\beta)]} \right\}.$$

2.6.5 Stability and Comparative Statics

In this section, we will carry out some analysis on the stability of the steady states. As our problem, (2.1)-(2.3), has two state variables, we have to investigate a four-dimensional system (two states and two co-states). So the Jacobian will be a 4x4-matrix, and hence the eigenvalues are the solutions of a fourth-degree polynomial. Therefore, it is hard to analyse the sign of the eigenvalues in general (note that our problem depends on seven parameters). We decided to simplify this analysis by holding six parameters fixed (at the values given in Section 2.4), and investigate the stability as well as the feasibility of the steady states depending on the remaining free parameter.

The analysis on the parameters a, b, γ, and ε leads to qualitatively similar results. For the parameters β and δ the results show slight differences to the ones just mentioned. The only parameter with significant differences in the results is r. Thus, in the following we will discuss the stability for the parameters γ (with short remarks on β and δ) and r.

Free Parameter: γ

As mentioned above, we fix all parameters except γ (so let $a = b = 1$, $r = 0.001$, $\beta = 0.005$, $\delta = 0.02$, $\varepsilon = 0.004$). Note, Proposition 2.6.2 guarantees that we have two steady states for all $\gamma > 0$ (if $r < 0.0041$, which is true in that case). So we plot the four eigenvalues, which are shown in Figure 2.10. We see that for all values of γ, two eigenvalues are positive (Figures 2.10(a) and (c)) while the others are negative (Figures 2.10(b) and (d)), both for the high and the low steady state. Hence, we have saddle-node stability for both.

In Figure 2.11, we see the GHG concentration, (a), and the GHG emissions, (b), as they depend on γ. We should note here that we do not show plots for the second state variable, the temperature, because they look like the plots for G with a different scale ($T^* = \varepsilon G^*$). Since $m > 0$ is necessary for feasibility, the higher steady state is not feasible (see Figure 2.11(b)), and so, the problem yields one stable and admissible steady state.

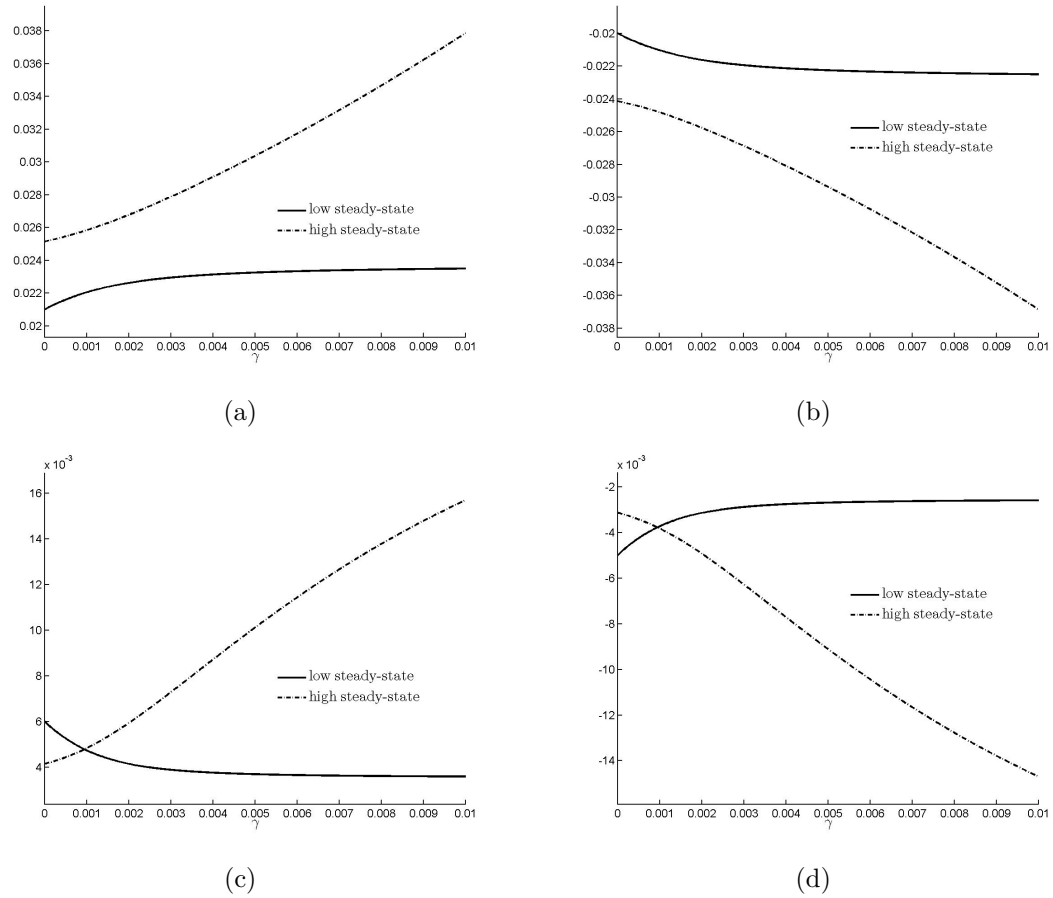

Figure 2.10: Eigenvalues for the lower and the higher steady state w.r.t. γ.

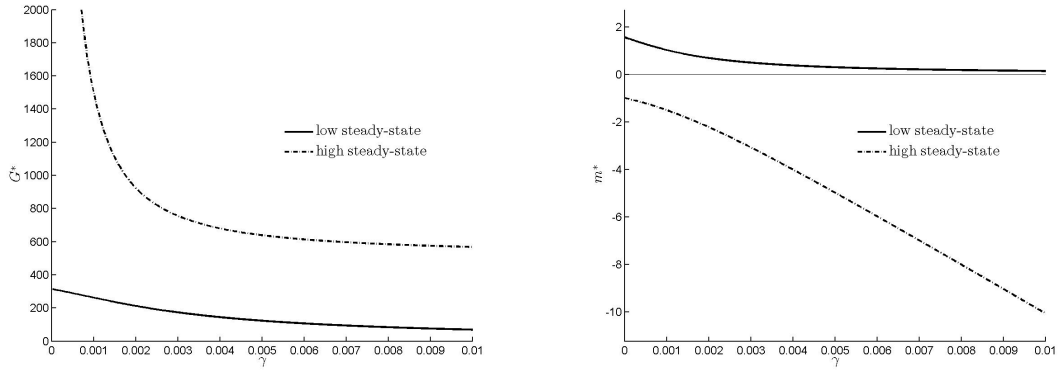

Figure 2.11: G and m for the lower and the higher steady state w.r.t. γ.

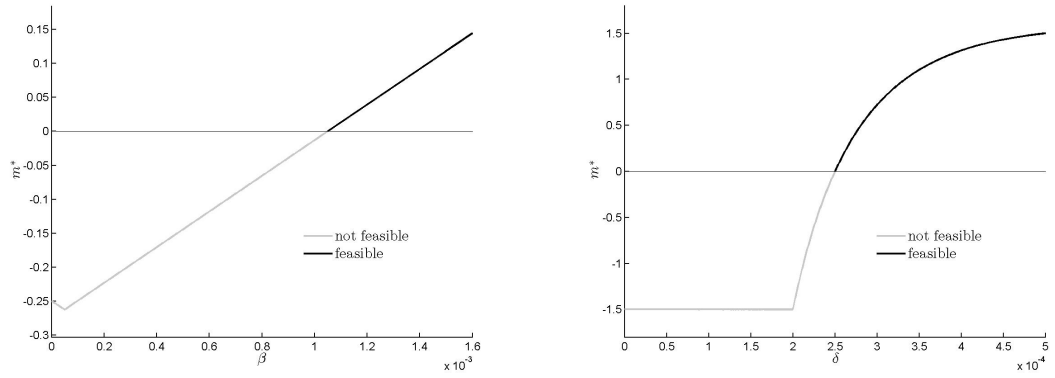

(a) (b)

Figure 2.12: m for the lower steady state w.r.t. β and δ.

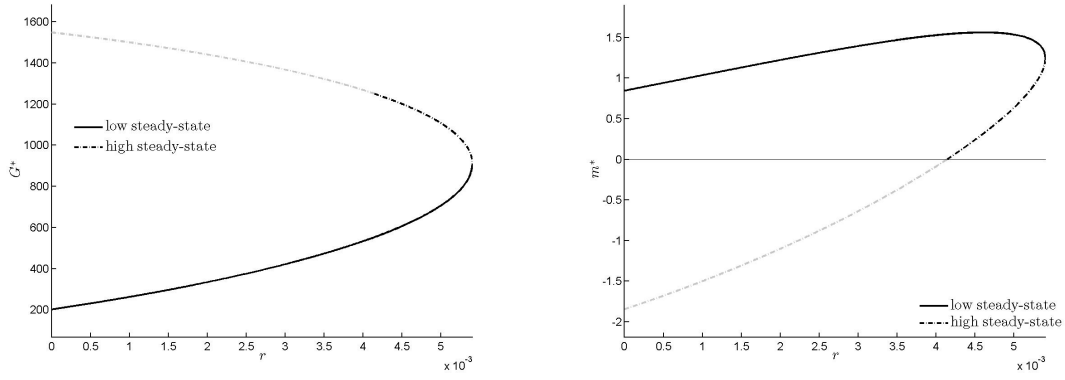

(a) G (b) m

Figure 2.13: G and m for the lower and the higher steady state w.r.t. r.

Cutouts of the control variable for small intervals of the parameters β and δ are shown in Figure 2.12. Here we see that for sufficiently small values even the lower steady state is not feasible. The rest is qualitatively similar to the results above.

Free Parameter: r

In this section we vary the parameter r and set $\gamma = 0.001$, while the other parameter values remain the same. First, we use Proposition 2.5 to study the existence of steady states. For the parameter values we chose, Proposition 2.5.1 guarantees two steady states for $r \in (0, 0.0054)$. If r is not within this interval, the problem yields one steady state for $r = 0.0054$, and we have no steady state otherwise. Hence, a so-called *blue-sky bifurcation* occurs in this case (see Grass et al. [10] for further information). This fact is also shown in Figure 2.13(a). In Figure 2.13(b) the steady-state GHG emissions are shown, and we see that the higher steady state becomes feasible for $r > 0.0041$, while it is not feasible

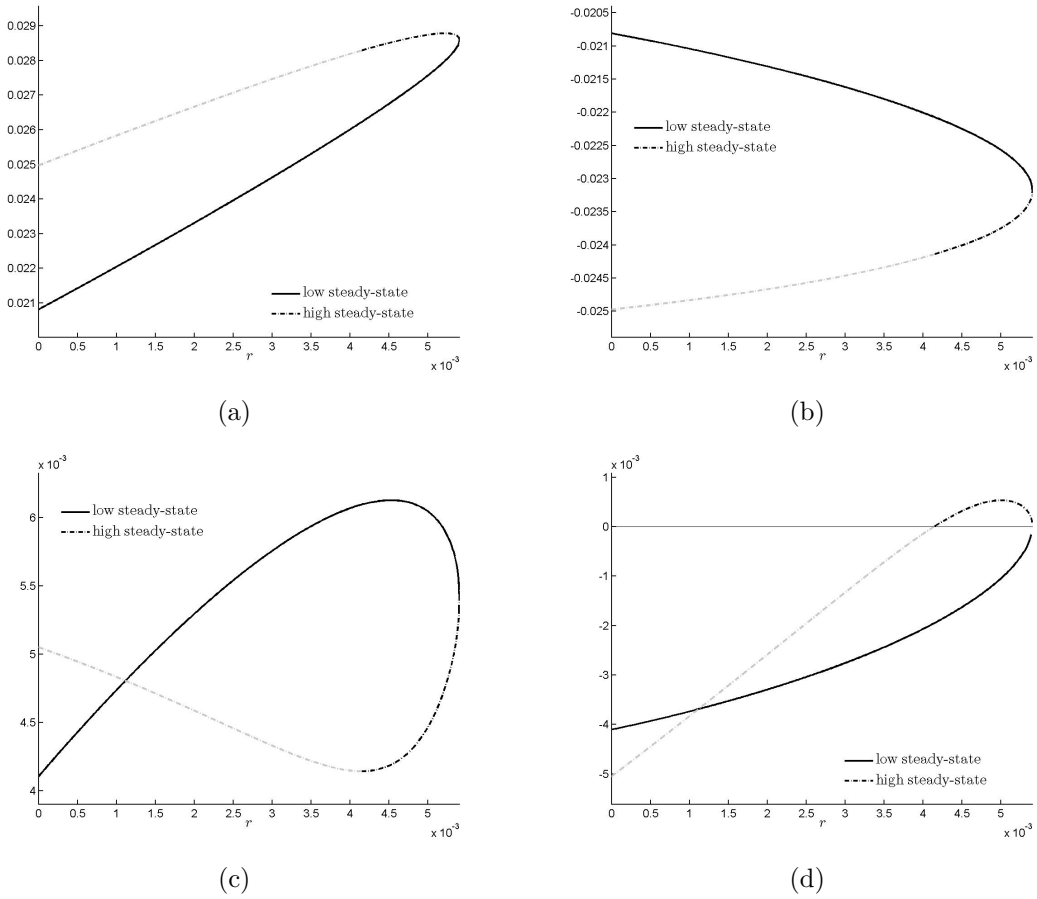

Figure 2.14: Eigenvalues for the lower and the higher steady state w.r.t. r.

for lower values of r. Note, in all plots within this section, the grey slice belongs to the non-feasible part, whereas the black slice belongs to the admissible parts of the steady states.

In Figure 2.14 we see again the four eigenvalues. While in (a)-(c) the signs of the eigenvalues do not change, the fourth eigenvalue of the higher steady state changes from negative to positive at the same parameter value as the higher steady state becomes admissible (Figure 2.14(d)). This means that as the higher steady state becomes feasible it changes its stability and becomes unstable (three eigenvalues greater than zero). We have a so-called *transcritical bifurcation* (more information can be found again in Grass et al. [10]).

Comparative Statics

In this section we derive comparative statics for all parameters. We only consider stable and feasible steady states. The easiest parameter to do this is the conversion parameter

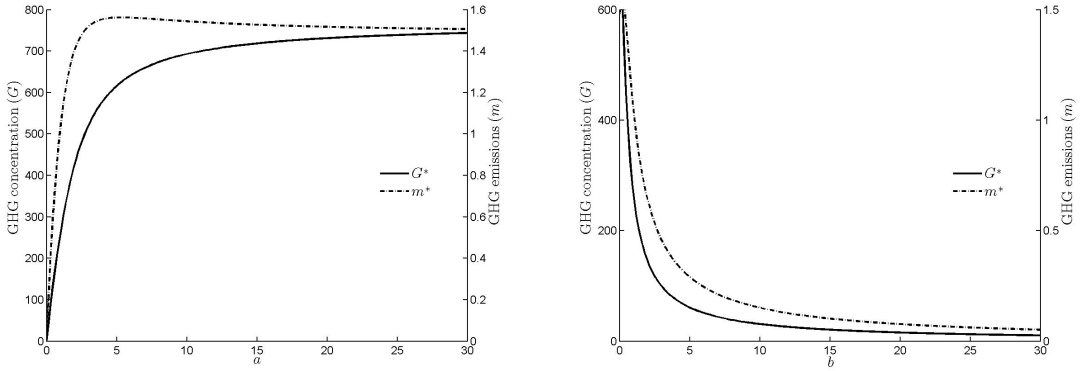

(a) Parameter a (b) Parameter b

Figure 2.15: G^* and m^* for the feasible and stable steady state w.r.t. the parameters a and b.

ε, which is the only parameter where we can derive analytical expressions. Let us define

$$C := \frac{1}{2\gamma}\left\{\frac{a\gamma(r+2\delta)}{b\delta} + \beta \pm \sqrt{\left[\beta + \frac{a\gamma(r+2\delta)}{b\delta}\right]^2 - \frac{4a\gamma(r+\beta)(r+\delta)}{b\delta}}\right\},$$

which does not depend on ε. Then (2.10) can be rewritten as $G^* = \frac{1}{\varepsilon}C$ and we get $\frac{\partial G^*}{\partial \varepsilon} = -\frac{1}{\varepsilon^2}C < 0$. For the optimal temperature we get $T^* = C$ and hence, $\frac{\partial T^*}{\partial \varepsilon} = 0$. From (2.12), the steady state control can be written as

$$m^* = \frac{1}{\varepsilon}\underbrace{\frac{a}{b\delta}\left[(r+\beta)(r+\delta) - \gamma(r+2\delta)C\right]}_{=:D},$$

and we compute $\frac{\partial m^*}{\partial \varepsilon} = -\frac{1}{\varepsilon^2}D$. Consequently, m (because for the parameter values we chose, $D > 0$ holds) and G decrease convex.y in the value of ε, and the temperature stays constant for all values of the parameter.

All the other parameters are analysed numerically. In Figure 2.15(a), we see that G^* and, hence, T^* increase concavely in the value of emissions, a, while the emissions at first increase quickly, but for larger values of a they begin to decrease. Note that in what follows we will only discuss the behaviour of the GHG concentration, because the temperature behaves alike. For the delay parameter, δ, the steady-state value of the control shows a similar behaviour (Figure 2.17(a)). However, the state variables for this parameter decrease in a convex way. The same effect occurs for both, the control and the state variables, in the value of the cost of global warming, b (Figure 2.15(b)), and the adjustment parameter of the absorption, γ (Figure 2.16(b)). For the decay parameter, β, the steady-state value of G^* stays constant at a level of about 262.5 billions of tons

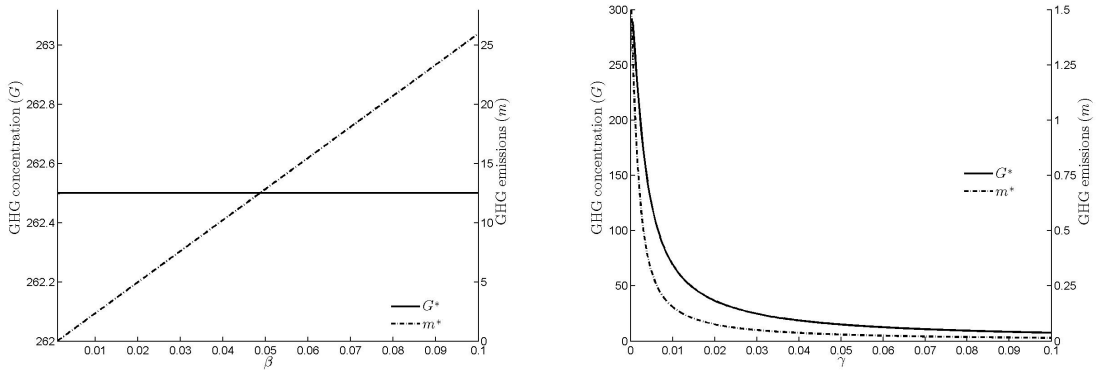

(a) Parameter β (b) Parameter γ

Figure 2.16: G^* and m^* for the feasible and stable steady state w.r.t. the parameters β and γ.

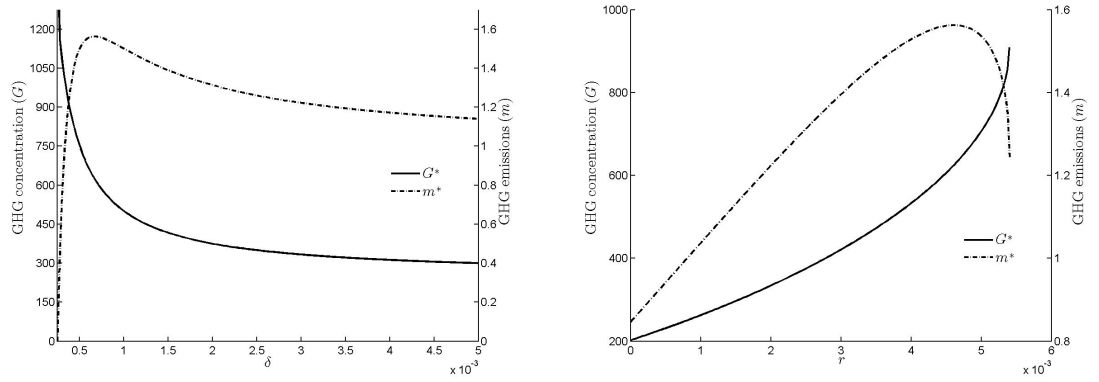

(a) Parameter δ (b) Parameter r

Figure 2.17: G^* and m^* for the feasible and stable steady state w.r.t. the parameters δ and r.

of CO_2 equivalent, while the emissions increase linearly (Figure 2.16(a)). An increase in the time preference rate, r, yields a convex increase in the GHG concentration, whereas the emissions at first increase towards a peak, to decrease from this value of r until the threshold where no longer a steady state exists (Figure 2.17(b)).

2.6.6 Is it Optimal to Head to the Steady State?

In this section we deal with the question, whether there is a path $(m(t), G(t), T(t))$, with $t > 0$, such that the objective function (2.3) yields a larger value than if we head to the steady state. We now assume that parameter values are chosen to yield a steady state for the problem and we further assume initial conditions $G(0) = G^*$ and $T(0) = T^*$, which also implies $m(0) = m^*$. This means, that the system constantly stays in equilibrium if

we choose $m(t) = m^*$, for all $t > 0$. Then the value of the objective function can be easily computed as

$$\int_0^\infty e^{-rt}(a \ln m(t) - bT(t))\, dt = \underbrace{\frac{1}{r}(a \ln m^* - bT^*)}_{=:E}.$$

However, a sufficient condition to get a higher value of the objective function is to choose

$$m(t) = \exp\left(\frac{E + bT(t)}{a}\right) + \kappa, \ \forall t > 0, \ \kappa > 0,$$

where κ is an arbitrarily positive constant. In this case, the system will explode, as in each time-step we choose the emissions high enough to compensate the penalty for the costs of global warming. As a consequence, the GHG concentration and the temperature will rise and in the next period the emissions get even higher.

The question remains, whether it is realistic that the emissions can become arbitrarily high. It may rather be reasonable to define an upper bound for m.

2.7 Summary

We now give a short overview of important results, which we found during the analyses of the Erickson model.

First, we studied a modification of the model by replacing the control variable by an exogenous level of emissions. We obtained that, depending on the parameter values, the system yields zero to two steady states. Interestingly only the lower equilibrium is stable, and the higher one is a saddle. The stable manifold of this steady state separates two areas. For initial values on the left side the system converges to the lower steady state, while for initial values on the right side the system explodes.

Also for the base model zero to two steady states exist. Unfortunately, because of the formulation of the model we could not derive sufficient optimality conditions. At least it was also possible to derive conditions, such that the lower equilibrium is a carbon sink. In the course of deriving comparative statics, we obtained that in most cases the lower steady state is stable and admissible, while the higher steady state is not admissible. For sufficiently low values of the parameters β and δ even the lower equilibrium is not stable. The system reacts differently due to changes in the discount rate. In that case bifurcation occurs. Another interesting fact is that there exists a range for r, such that the higher steady state becomes admissible, but unstable.

An important conclusion of this chapter is also that the influence of the "quadratic"

parameter is essential for the complexity of the problem. If we omit this parameter from the system by setting it equal to zero, the model simplifies and yields one unique steady state.

Chapter 3

The Greiner et al. Model

In this chapter we present the model of Greiner and Semmler [3] respectively Greiner et al. [4]. The goal is to analyse and understand the model, because we later want to combine it with Erickson's model of Chapter 2. In the course of the analyses, we will use the `Matlab` toolbox `OCMat`.

3.1 Dynamics of the GHG Concentration due to Anthropogenic Emissions and the Average Surface Temperature of Earth

In this section we derive differential equations for the dynamics of the environment. Therefore, also interactions between temperature increase and GHG emissions will be considered. We follow Greiner and Semmler [3] (Section 2) respectively Greiner et al. [4] (Section 2).

One of the simplest methods to model the climate system is by using so-called *energy balance models* (EBM). These models describe changes in the climate system of the earth in terms of its global energy balance. According to an EBM we can write

$$\dot{T}(t)\, c_h = S_E - H(t) - F_N(t),$$

where $T(t)$ is the average global surface temperature of the earth at time t (for reasons of simplicity the time argument will be omitted in the following) measured in Kelvin (K)[1] and c_h is the heat capacity[2] in units of $\mathrm{J\,m^{-2}\,K^{-1}}$ (Joule per square meter per Kelvin).

[1] 273 K equals 0 °C.

[2] This means the amount of heat that is needed to be added per $\mathrm{m^2}$ of horizontal area to raise the surface temperature by 1 K.

The solar input is given by S_E, H is the non-radiative energy flow, and F_N is the difference between the outgoing $F\uparrow$ and the incoming radiative flux $F\downarrow$, so

$$F_N = F\uparrow - F\downarrow.$$

All three variables mentioned above are given in units of $\mathrm{W\,m^{-2}}$ (Watt per square meter). The outgoing radiative flux, $F\uparrow$, follows the Stefan-Boltzmann law given by

$$F\uparrow = \zeta\,\sigma_T\,T^4,$$

where ζ denotes the emissivity (which is the ratio of actual emissions of a body to the emissions of a blackbody[3]). For the earth we can set $\zeta = 0.95$. The parameter σ_T is the so-called Stefan-Boltzmann constant and we assume[4] a value of $\sigma_T = 5.67\ 10^{-8}\,\mathrm{W\,m^{-2}\,K^{-4}}$. Along with the ratio $\frac{F\uparrow}{F\downarrow} = \frac{109}{88}$, this leads to

$$\begin{aligned} F_N &= \frac{21}{109}\,F\uparrow = \frac{21}{109}\,\zeta\,\sigma_T\,T^4 = \\ &= \frac{1.131165}{1.09\cdot 10^8}\,T^4. \end{aligned}$$

The difference between the solar input and the non-radiative energy flow can be written as

$$S_E - H = \frac{1}{4}\,Q(1-\alpha_1(T)),$$

where Q is the solar constant and we assume that $Q = 1367.5\ \mathrm{W\,m^{-2}}$ holds. The function $\alpha_1(T)$, the planetary albedo, describes the reflecting power of the earth, which depends negatively on the average surface temperature. This factor takes effect because with rising temperature some feedback effects occur which likely affect the amount of energy reflected by earth. Two examples are the ice albedo feedback mechanism and the water vapour *greenhouse* effect. The ice albedo, for instance, means that a higher surface temperature will reduce areas with ice and snow and as these are important factors of reflecting energy, more solar radiation stays within our atmosphere. Moreover, an increase of the surface temperature also implies a higher concentration of water vapour in the atmosphere. Therefore, a rise of the greenhouse effect will be the consequence because water vapour is the dominant GHG.

So, the function $1-\alpha_1(T)$ describes the fraction of the energy which is not reflected

[3]For blackbodies, $\zeta = 1$ holds.

[4]The exact value relying on current measuring accuracy is $\sigma_T = (5.670373 \pm 0.000021)\ 10^{-8}\ \mathrm{W\,m^{-2}\,K^{-4}}$.

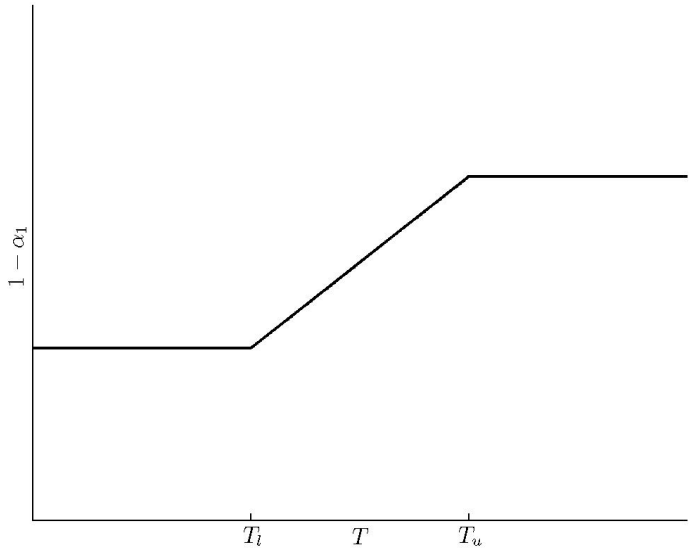

Figure 3.1: A function $1-\alpha_1(T)$ should look like.

and stays within the atmosphere. In Figure 3.1, a function is shown as proposed by Greiner and Semmler [3] for $1-\alpha_1(T)$. If the temperature lies under the lower bound T_l or above the upper bound T_u, the albedo is a constant, while between these values $\alpha_1(T)$ declines in a linear way, and therefore $1-\alpha_1(T)$ increases. For the mathematical analysis we will approximate the function shown in Figure 3.1 by a differentiable function which is given by

$$1-\alpha_1(T) = k_1 \frac{2}{\pi} \arctan\left(\frac{\pi(T-293)}{2}\right) + k_2. \tag{3.1}$$

The parameters k_1 and k_2 are set to $k_1 = 5.6\ 10^{-3}$ and $k_2 = 0.2135$. In Figure 3.2 the function is shown for these parameter values. For the pre-industrial level of about 287.8 K the amount which is not reflected is $1-\alpha_1(T) = 0.2083$.

Summing up, the EBM yields

$$\dot{T}\, c_h = \frac{1367.5}{4}\,(1-\alpha_1(T)) - \frac{1.131165}{1.09\cdot 10^8}\,T^4. \tag{3.2}$$

Because the earth's surface is largely covered by seawater, the oceans highly influence the heat capacity, c_h, of our planet. Hence, we take the heat capacity of the oceans and use it as a proxy for c_h. We follow Greiner and Semmler [3] and set $c_h = 0.1497$.

Next, we want to work out the effect of emitted GHGs onto our climate system. This is needed, because an increase in the GHG concentration due to anthropogenic emissions also reinforces the greenhouse effect. Hence, we calculate the so-called *radiative forcing*,

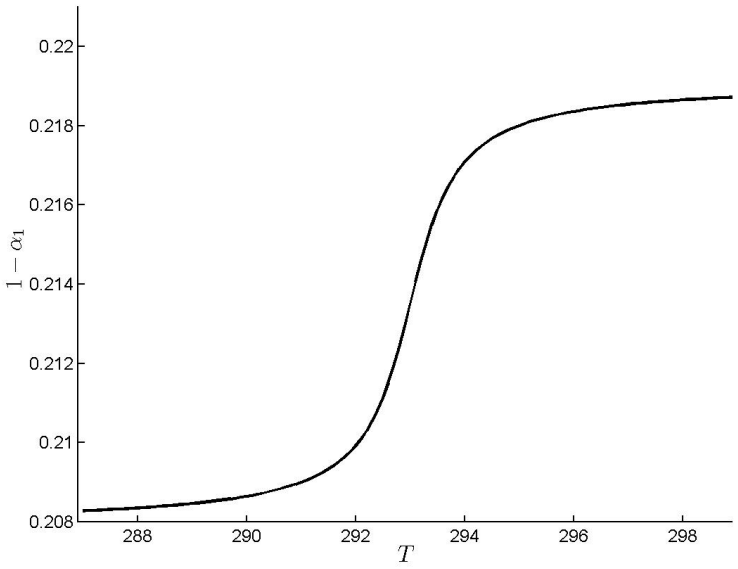

Figure 3.2: Approximation of the function given in Figure 3.1 by using equation (3.1) with parameter values $k_1 = 5.6\ 10^{-3}$ and $k_2 = 0.2135$.

which is a measure of the influence of a GHG onto the balance of incoming and outgoing energy of the atmosphere. Regarding CO_2, the radiative forcing is

$$F = 6.3\ \ln \frac{M}{M_{pre}}, \tag{3.3}$$

which is measured in $\mathrm{W\,m^{-2}}$. In (3.3), M is the actual CO_2 concentration, and M_{pre} denotes the pre-industrial CO_2 concentration. For all other GHGs, similar formula can be calculated, but as we convert all GHGs into CO_2 equivalents, we are only interested in the radiative forcing of CO_2. Integrating (3.3) in (3.2) yields

$$\dot{T}\, c_h = \frac{1367.5}{4}\,(1 - \alpha_1(T)) - \frac{1.131165}{1.09 \cdot 10^8}\,T^4 + \beta_1\,(1-\xi)\,6.3\,\ln\frac{M}{M_{pre}}$$

with the initial condition $T(0) = T_0$. The parameter ξ takes into account that a portion of the warmth due to the GHG effect is absorbed by the oceans, and β_1 describes the fact that with a higher GHG concentration, and therefore a higher average surface temperature, the absorption effect is reduced. We assume $\xi = 0.3$ and $\beta_1 = 1.1$.

Finally, we state the dynamics of the GHG concentration, M, which follows the differential equation

$$\dot{M} = \beta_2\, E - \mu_1\, M \tag{3.4}$$

with initial condition $M(0) = M_0$. In (3.4), E denotes the emissions which increase the GHG concentration, but a part of it is again absorbed by the oceans and does not enter the atmosphere (this part is given by $1 - \beta_2$). The parameter μ_1 is the inverse of the lifetime of CO_2, and therefore $\mu_1 M$ describes the portion of GHG concentration which is decomposed. The parameters are set to $\mu_1 = 0.1$ and, according to the IPCC [11], $\beta_2 = 0.49$.

3.2 Description of the Underlying Economy

In this model we consider an economy where one homogenous good is produced. Furthermore, all individuals respectively households are assumed to be identical. As decision maker, we consider a social planner who will take into account both, benefits as well as negative effects on the environment.

We assume that production is based on only one input factor, capital, where the production function should be an AK model modified by a damage function:

$$y = B\, k\, D_2(T). \tag{3.5}$$

In the equation above, y denotes the per capita production and k the per capita capital. The parameter B is a positive constant, which we set to $B = 0.35$, and $D_2(T)$ denotes the damage function mentioned above. This function measures the negative effect on the output if the temperature increases over the pre-industrial level (which is $T_{pre} = 287.8$ K). We assume the functional form of the damage function as

$$D_2(T) = \left[a_1 \left(T - T_{pre}\right)^2 + 1\right]^{-\psi}, \tag{3.6}$$

with the constants $a_1 > 0$ and $\psi > 0$. According to the IPCC 1995 [12], a doubling of GHGs, which corresponds to a temperature increase between 1.5 and 4.5 degrees, implies a reduction of world GDP by 1.5 to 2 percent. So, we assume $a_1 = 0.04$ and $\psi = 0.05$, which implies that an increase in surface temperature by 3 $(2; 1)$ degrees denotes a damage of 1.5 $(0.7; 0.2)$ percent.

The budget constraint of the social planner is given by

$$\begin{aligned} \dot{k} &= y - c - a - (\delta + n)\, k \\ &= B\, k\, D_2(T) - c - a - (\delta + n)\, k \end{aligned}$$

with c denoting the per capita consumption and a being per capita abatement spending. The parameters δ and n denote the depreciation rate of capital respectively the growth

rate of labour force, and we assume $\delta = 0.075$ and $n = 0.02$.

Further, we suppose a logarithmic utility function for the representative household which only depends on per capita consumption:

$$U(c) = \ln c.$$

The goal of the social planner is to maximise the discounted utility of all households, which yields the objective function

$$\max_{c,a} \int_{t=0}^{\infty} e^{-\rho t} L_0 e^{nt} U(c) \; dt.$$

The labour supply at time $t = 0$ is given by L_0 and can be normalised to 1, and we assume exponential growth of labour force at rate n (as mentioned above). The discount rate is given by ρ which we assume to be 0.03. Keep in mind that the variables k, c, and a actually have a time argument, which has been omitted for the sake of convenience. The other variables denote parameters and are constant over time.

For the GHG emissions we assume that they occur as by-products of the capital used in production, and all emissions will be stated in terms of CO_2 equivalents. So, with higher capital spending, the GHG emissions will rise. However, the emissions can be reduced by abatement spending. Summing up, this means that the function denoting emissions has to fulfill the following properties:

$$\begin{aligned} &E \equiv E(k, a), \\ &\frac{\partial E}{\partial k} > 0, \; \frac{\partial E}{\partial a} < 0. \end{aligned}$$

We should mention here that emissions do not affect the production directly, but only indirectly due to their impact onto the GHG concentration (see Equation (3.4)) and thus, onto the temperature. As a function, which takes into account the assumptions mentioned above, we consider

$$E = \left(\varepsilon \, \frac{k}{a} \right)^{\gamma}, \tag{3.7}$$

and we consider $\varepsilon > 0$ and $\gamma > 0$. The parameter ε can be interpreted as a technology index, describing how polluting the underlying technology is. A higher parameter induces a more polluting technology (for a fixed amount of capital and abatement) and vice versa. As parameter values we assume $\varepsilon = 1.65 \; 10^{-4}$ and $\gamma = 1$.

3.3 The Model

Bringing the preceding two sections together leads us to the following infinite-horizon optimal control model with two control and three state variables:

$$\begin{aligned}
\max_{c,a} \ & \int_{t=0}^{\infty} e^{-\rho t} L_0 e^{nt} \ln c \ dt, \\
\text{s.t. } & \dot{k} = B\, k\, D_2(T) - c - a - (\delta + n)\, k, \\
& \dot{T}\, c_h = \frac{1367.5}{4}\,(1 - \alpha_1(T)) - \frac{1.131165}{1.09 \cdot 10^8}\, T^4 + \beta_1\,(1-\xi)\,6.3\,\ln\frac{M}{M_{pre}}, \\
& \dot{M} = \beta_2\, E - \mu_1\, M, \\
& T(0) = T_0, M(0) = M_0, k(0) = k_0,
\end{aligned} \tag{3.8}$$

which has to be solved by the social planner. The function $D_2(T)$ is given by (3.6), E is given by (3.7), and $1 - \alpha_1(T)$ by (3.1). As mentioned before, the initial labour force is set to $L_0 = 1$, and also the pre-industrial level of GHG concentration is normalised to 1 ($M_{pre} = 1$).

3.3.1 Optimisation

To derive the optimal solution we formulate the current-value Hamiltonian, given by

$$\begin{aligned}
H(\cdot) = \ln c + \lambda_1 \left[B\, k\, D_2(T) - c - a - (\delta + n)\, k\right] + \\
\lambda_2 \left[\frac{1367.5}{4}\,(1 - \alpha_1(T)) - \frac{1.131165}{1.09 \cdot 10^8}\, T^4 + \beta_1\,(1-\xi)\,6.3\,\ln M\right]\frac{1}{c_h} + \\
\lambda_3 \left[\beta_2 \left(\varepsilon\,\frac{k}{a}\right)^{\gamma} - \mu_1 M\right].
\end{aligned}$$

Similar to the control and state variables, also the shadow prices, λ_1, λ_2, and λ_3 have a time argument which we have omitted. Note that the shadow price of capital is positive, while the ones of the temperature and the GHG concentration are negative. The first-

order conditions are given by

$$\frac{\partial H(\cdot)}{\partial c} = \frac{1}{c} - \lambda_1 \stackrel{!}{=} 0, \tag{3.9a}$$

$$\frac{\partial H(\cdot)}{\partial a} = -\lambda_3\,\beta_2\,\gamma\,\varepsilon^{\gamma}\,k^{\gamma}\,a^{-\gamma-1} - \lambda_1 \stackrel{!}{=} 0, \tag{3.9b}$$

$$\dot{\lambda}_1 = \lambda_1(\rho + \delta - B\,D_2(T)) - \lambda_3\,\beta_2\,\gamma\,\left(\frac{\varepsilon}{a}\right)^{\gamma}\,k^{\gamma-1}, \tag{3.9c}$$

$$\dot{\lambda}_2 = \lambda_2\left[\rho - n + \frac{1}{c_h}\left(\frac{1367.5}{4}\alpha_1'(T) + \frac{4.52466}{1.09\cdot 10^8}T^3\right)\right] - \lambda_1\,B\,k\,D_2'(T), \tag{3.9d}$$

$$\dot{\lambda}_3 = \lambda_3(\rho - n + \mu_1) - \lambda_2\frac{\beta_1\,(1-\xi)\,6.3}{c_h\,M}.$$

Further, the transversality condition $\lim_{t\to\infty} e^{-(\rho-n)t}(\lambda_1\,k + \lambda_2\,T + \lambda_3\,M) = 0$ must hold.

In (3.9d), $D_2'(T)$ and $\alpha_1'(T)$ denote the derivatives w.r.t. T. These two expressions are given by

$$D_2'(T) = -2\psi\frac{a_1\,(T-287.8)}{\left[a_1\,(T-287.8)^2+1\right]^{1+\psi}}, \tag{3.10}$$

$$\alpha_1'(T) = -\frac{k_1}{1+\frac{\pi^2}{4}(T-293)^2}. \tag{3.11}$$

By calculating the first derivative of (3.9a) w.r.t. t and using the fact that (3.9a) implies $c = \lambda_1^{-1}$, we obtain

$$\dot{c} = -c\frac{1}{\lambda_1}\dot{\lambda}_1. \tag{3.12}$$

Further, from (3.9a) and (3.9b) we compute

$$a = \left(-\lambda_3\,\beta_2\,\gamma\,\varepsilon^{\gamma}\frac{c}{k}\right)^{-\frac{\gamma}{1+\gamma}}\,k^{-\gamma}. \tag{3.13}$$

By using (3.9a), (3.9c), (3.12), and (3.13) we get the following canonical system of au-

tonomous differential equations, which describes the dynamics of the problem:

$$\dot{c} = c\left[-(\rho+\delta) + B\,D_2(T) - \left(-\lambda_3\,\beta_2\,\gamma\,\varepsilon^\gamma\frac{c}{k}\right)^{\frac{1}{1+\gamma}}\right], \tag{3.14a}$$

$$\dot{k} = k\left[B\,D_2(T) - \frac{c}{k} - \left(-\lambda_3\,\beta_2\,\gamma\,\varepsilon^\gamma\frac{c}{k}\right)^{\frac{1}{1+\gamma}} - (\delta+n)\right], \tag{3.14b}$$

$$\dot{T} = \frac{1}{c_h}\left[\frac{1367.5}{4}\left(1-\alpha_1(T)\right) - \frac{1.131165}{1.09\cdot 10^8}\,T^4 + \beta_1\,(1-\xi)\,6.3\,\ln M\right], \tag{3.14c}$$

$$\dot{M} = \left\{\beta_2\left[\frac{\varepsilon\,k}{(-\lambda_3)\,\gamma\,c}\right]^\gamma\right\}^{\frac{1}{1+\gamma}} - \mu_1\,M, \tag{3.14d}$$

$$\dot{\lambda}_2 = \lambda_2\left[\rho - n + \frac{1}{c_h}\left(\frac{1367.5}{4}\alpha_1'(T) + \frac{4.52466}{1.09\cdot 10^8}T^3\right)\right] - B\,D_2'(T)\frac{k}{c}, \tag{3.14e}$$

$$\dot{\lambda}_3 = \lambda_3(\rho - n + \mu_1) - \lambda_2\,\frac{\beta_1\,(1-\xi)\,6.3}{c_h\,M}. \tag{3.14f}$$

If we now substitute $\tilde{c} \equiv \frac{c}{k}$, we get

$$\dot{\tilde{c}} = \tilde{c}\left(\frac{\dot{c}}{c} - \frac{\dot{k}}{k}\right) \overset{(3.14a),(3.14b)}{=} \tilde{c}\,\left[\tilde{c} - (\rho - n)\right]. \tag{3.15}$$

That means, the system (3.14) can be reduced to (3.14c)-(3.14f) and (3.15).

Definition 3.1 (BGP1)**.** *A balanced growth path (BGP) is a path such that* $\dot{T} = 0$*,* $\dot{M} = 0$*, and* $\dot{\tilde{c}} = 0$ *hold, with* $M \geq M_{pre}$*.*

Remark. *Note that*

1. $\dot{\tilde{c}} = 0$ *is equivalent to* $\frac{\dot{c}}{c} = \frac{\dot{k}}{k}$*, so along a BGP we have growth in capital and consumption, and both growth rates are the same;*
2. *with* $\dot{T} = \dot{M} = 0$ *also* $\dot{\lambda}_2 = \dot{\lambda}_3 = 0$ *holds; and*
3. *we require* $M \geq M_{pre}$ *for reasons of realism (only a GHG concentration larger than the pre-industrial level is realistic).*

To derive a steady state we solve the system $\dot{\tilde{c}} = \dot{T} = \dot{M} = \dot{\lambda}_2 = \dot{\lambda}_3 = 0$ and hence, we proceed as follows. From (3.15) we obtain that $\tilde{c} = \rho - n$ holds on the BGP. We now define some variables, which we use in the following passage for the ease of readability

and to provide a clear overview:

$$\begin{aligned}\omega_1 &= \rho - n,\\ \omega_2 &= 6.3\,\beta_1\,(1-\xi),\\ \omega_3 &= \frac{1367.5}{4},\\ \omega_4 &= \frac{1.131165}{1.09\cdot 10^8}.\end{aligned}$$

Then, we set $\dot{M} = 0$ and transform the obtained equation to the form $M \equiv M(\lambda_3, \cdot)$, which leads to

$$M = \frac{1}{\mu_1}\left[\beta_2\left(-\frac{\varepsilon}{\lambda_3\,\gamma\,\omega_1}\right)^{\gamma}\right]^{\frac{1}{1+\gamma}}. \tag{3.16}$$

Here, $M(\lambda_3, \cdot)$ denotes a function of λ_3 and parameters, which do not depend on t. Next, we set $\dot{\lambda}_3 = 0$ and use (3.16). The obtained expression can be written as $\lambda_2 \equiv \lambda_2(\lambda_3, \cdot)$ and is given by

$$\lambda_2 = -(\omega_1+\mu_1)\,\left[-\lambda_3\,\beta_2\,\left(\frac{\varepsilon}{\gamma\,\omega_1}\right)^{\gamma}\right]^{\frac{1}{1+\gamma}}\,\frac{c_h}{\omega_2\,\mu_1}.$$

Setting $\dot{T} = 0$ together with (3.16) yields an expression which can be transformed to the form $\lambda_3 \equiv \lambda_3(T, \cdot)$ and explicitly is given by

$$\lambda_3 = -\left[\exp\left(\frac{\omega_4\,T^4 - \omega_3\,(1-\alpha_1(T))}{\omega_2}\right)\mu_1\right]^{-\frac{1+\gamma}{\gamma}}\,\frac{\varepsilon}{\gamma\,\omega_1}\,\beta_2^{\frac{1}{\gamma}}. \tag{3.17}$$

Hence, we get $\lambda_2 \equiv \lambda_2(T, \cdot)$ by

$$\lambda_2 = -\frac{(\omega_1+\mu_1)\,\varepsilon\,c_h}{\gamma\,\omega_1\,\omega_2}\,\left[\frac{\mu_1^{1+\gamma}}{\beta_2}\exp\left(\frac{\omega_4\,T^4 - \omega_3\,(1-\alpha_1(T))}{\omega_2}\right)\right]^{-\frac{1}{\gamma}}. \tag{3.18}$$

Finally, we insert the last expression into $\dot{\lambda}_2$ and get a differential equation which only depends on T. This differential equation is given by

$$\begin{aligned}\dot{\lambda}_2 = &-\frac{(\omega_1+\mu_1)\,\varepsilon\,c_h}{\gamma\,\omega_1\,\omega_2}\,\left[\frac{\mu_1^{1+\gamma}}{\beta_2}\exp\left(\frac{\omega_4\,T^4 - \omega_3\,(1-\alpha_1(T))}{\omega_2}\right)\right]^{-\frac{1}{\gamma}}\cdot\\ &\left(\omega_1 + \frac{\omega_3\,\alpha_1'(T) + 4\,\omega_4\,T^3}{c_h}\right) - \frac{B\,D_2'(T)}{\omega_1}.\end{aligned} \tag{3.19}$$

Therefore, a solution T^* of $\dot{\lambda}_2 = 0$ gives a steady state. The remaining steady-state

variables can be computed by $\lambda_2^* = \lambda_2(T^*, \cdot)$, $\lambda_3^* = \lambda_3(T^*, \cdot)$, and $M^* = M(\lambda_3^*, \cdot)$, compare Equations (3.18), (3.17), and (3.16). Note, we cannot derive steady-state values for c and k, but for their proportion, $\tilde{c}$.

3.3.2 Numerical Analysis

Because of the complexity of the model, we cannot derive a solution analytically. Hence, we use the parameter values we introduced in the previous sections, which are summed up and shortly described in Table 3.1. In Figure 3.3, the function $\dot{\lambda}_2(T)$ is shown for these values, and the steady state is given where the curve intersects the $\dot{\lambda}_2 = 0$ line. Note that we only examine the range for values $T \geq T_{pre} = 287.8$, as a lower steady state does not seem to be a realistic scenario. As we see, the problem yields one steady state at $T^* = 287.9$. Although in Figure 3.3 we only plotted a range for T lower than 320, we also investigated higher (very unrealistic) ranges up to an upper bound of 4000, and the obtained steady state was still unique. We suppose that $\dot{\lambda}_2$ has no more zeros, but unfortunately the expression is too complicated to prove that there is actually only one steady state for $T \geq T_{pre}$. However, what we can show is that the function converges to zero. See Appendix B.1 for the technical details.

Based on $T^* = 287.9$, the corresponding value for the GHG concentration is $M^* = 1.02$. So, in equilibrium, we observe an increase in temperature of 0.1 degrees and an increase of the GHG concentration of 2 percent over the preindustrial level. We have summed up the steady-state values together with the eigenvalues of the Jacobian in Table 3.2. Hence, the steady state is saddle-point stable (two negative and two positive eigenvalues).

3.4 The Modified Model

In the preceding section we presented an economic growth model with constant returns to scale (as a consequence, $\dot{c}$ and $\dot{k}$ did not converge). In this section, we will transform the model into a model with decreasing returns to scale w.r.t. capital, k. Therefore, we change the output of the economy, given in (3.5), to

$$y = B\, k^{\alpha}\, D_2(T),$$

Parameter	Value	Description
ρ	0.03	discount rate
n	0.02	growth rate of labour force
L_0	1	labour force at time $t = 0$
B	0.35	constant, scaling the production function
T_{pre}	287.8	pre-industrial surface temperature
δ	0.075	depreciation rate of capital
c_h	0.1497	heat capacity
β_1	1.1	implies that a higher GHG concentration means less warmth absorption
ξ	0.3	fraction of the warmth increase which is absorbed by the ocean
M_{pre}	1	pre-industrial CO_2 concentration
β_2	0.49	denotes that a certain part of emissions do not enter the atmosphere
μ_1	0.1	inverse of atmospheric lifetime of CO_2
ε	$1.65\ 10^{-4}$	technology index
γ	1	constant of the emission function
k_1	$5.6\ 10^{-3}$	constant in the function of the albedo
k_2	0.2135	constant in the function of the albedo
a_1	0.04	constant in the damage function
ψ	0.05	constant in the damage function

Table 3.1: Overview of the values and descriptions for the parameters used to numerically analyse the model given in (3.8).

$\tilde{c}^*$	T^*	M^*	Eigenvalues
0.01	287.9	1.02	6.41, −6.4, −0.48, 0.49

Table 3.2: Steady-state values.

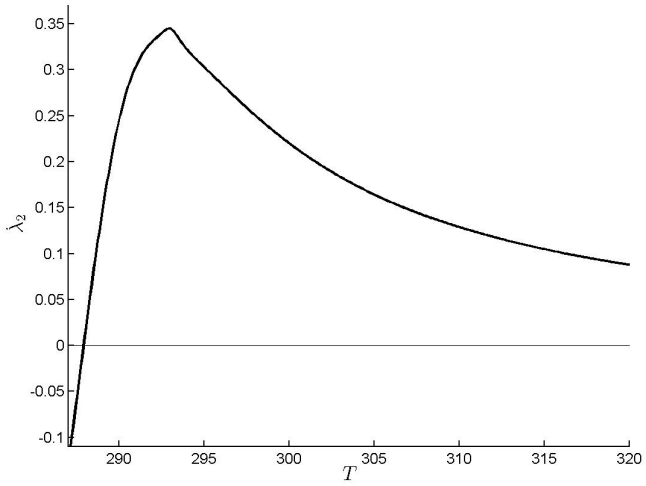

Figure 3.3: Segment of the $\dot{\lambda}_2$-curve for parameter values summarised in Table 3.1. The function has one zero at $T = 287.9$.

with α denoting the capital share, for which we assume $0 < \alpha < 1$. Then, the optimal control problem is given by

$$\max_{c,a} \int_{t=0}^{\infty} e^{-\rho t} L_0 e^{nt} \ln c \; dt, \tag{3.20a}$$

$$\text{s.t. } \dot{k} = B\, k^{\alpha}\, D_2(T) - c - a - (\delta + n)\, k, \tag{3.20b}$$

$$\dot{T}\, c_h = \frac{1367.5}{4}\,(1 - \alpha_1(T)) - \frac{1.131165}{1.09 \cdot 10^8}\, T^4 + \beta_1\,(1-\xi)\,6.3\,\ln\frac{M}{M_{pre}}, \tag{3.20c}$$

$$\dot{M} = \beta_2 \left(\varepsilon\,\frac{k}{a}\right)^{\gamma} - \mu_1\, M, \tag{3.20d}$$

$$T(0) = T_0, M(0) = M_0, k(0) = k_0.$$

Note, the model we presented in the previous section is a special case of the current model for $\alpha = 1$.

3.4.1 Optimisation

First, as before we normalise the initial labor force as well as the pre-industrial level of GHG concentration to unity. To derive an optimal solution, we next formulate the current-value Hamiltonian, which is given by

$$\begin{aligned} H(\cdot) = \ln c + \lambda_1 \left[B\, k^{\alpha}\, D_2(T) - c - a - (\delta + n)\, k\right] + \\ \lambda_2 \left[\frac{1367.5}{4}\,(1 - \alpha_1(T)) - \frac{1.131165}{1.09 \cdot 10^8}\, T^4 + \beta_1\,(1-\xi)\,6.3\,\ln M\right]\frac{1}{c_h} + \\ \lambda_3 \left[\beta_2 \left(\varepsilon\,\frac{k}{a}\right)^{\gamma} - \mu_1 M\right]. \end{aligned}$$

Hence, the necessary first-order conditions are:

$$\frac{\partial H(\cdot)}{\partial c} = \frac{1}{c} - \lambda_1 \stackrel{!}{=} 0, \tag{3.21a}$$

$$\frac{\partial H(\cdot)}{\partial a} = -\lambda_3\,\beta_2\,\gamma\,(\varepsilon\,k)^{\gamma}\; a^{-\gamma-1} - \lambda_1 \stackrel{!}{=} 0, \tag{3.21b}$$

$$\dot{\lambda}_1 = \lambda_1 \left(\rho + \delta - \alpha\, B\, k^{\alpha-1}\, D_2(T)\right) - \lambda_3\,\beta_2\,\gamma \left(\frac{\varepsilon}{a}\right)^{\gamma} k^{\gamma-1}, \tag{3.21c}$$

$$\dot{\lambda}_2 = \lambda_2 \left[\rho - n + \frac{1}{c_h}\left(\frac{1367.5}{4}\alpha_1'(T) + \frac{4.52466}{1.09 \cdot 10^8} T^3\right)\right] - \lambda_1\, B\, k^{\alpha}\, D_2'(T), \tag{3.21d}$$

$$\dot{\lambda}_3 = \lambda_3(\rho - n + \mu_1) - \lambda_2 \frac{\beta_1\,(1-\xi)\,6.3}{c_h\, M}. \tag{3.21e}$$

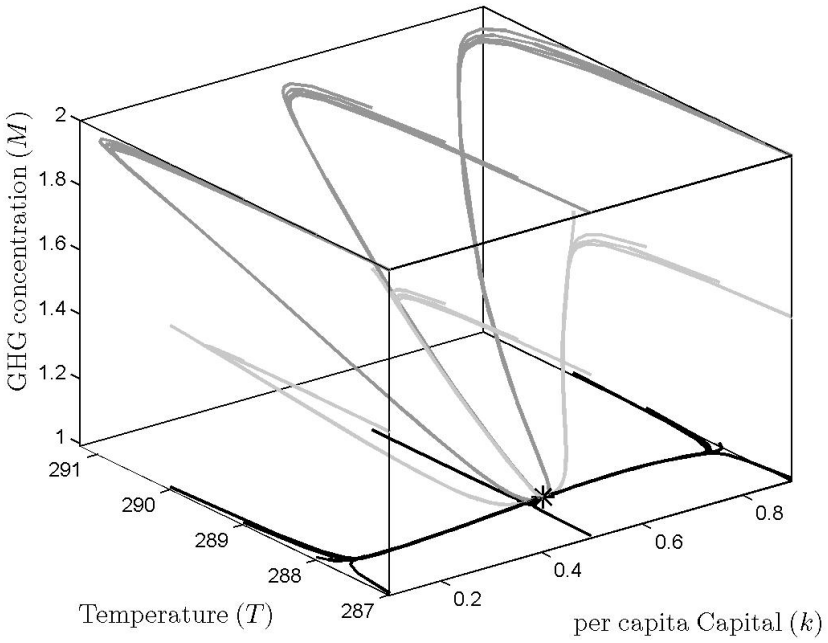

Figure 3.4: Phase portrait of (3.20) in the (k, T, M)-space. Black arcs show trajectories for initial values with $M(0) = 1$, for the light-grey curves $M(0) = 1.5$ hold, and the dark-grey ones satisfy $M(0) = 2$.

From (3.21a) and (3.21b) we obtain

$$c = \frac{1}{\lambda_1} \text{ and} \tag{3.22}$$

$$a = \left(-\frac{\lambda_3 \, \beta_2 \, \gamma \, \varepsilon^\gamma \, k^\gamma}{\lambda_1} \right)^{\frac{1}{1+\gamma}} . \tag{3.23}$$

Then, the system of ordinary differential equations given by (3.20b)-(3.20d) and (3.21c)-(3.21e) together with the equations (3.22) and (3.23) describes the optimal behaviour of the problem. To derive steady states we have to solve the system $\dot{k} = \dot{T} = \dot{M} = \dot{\lambda}_1 = \dot{\lambda}_2 = \dot{\lambda}_3 = 0$.

3.4.2 Numerical Analysis

The results presented in the following were computed by using the `Matlab` toolbox `OCMat`. The parameter values are the same as in Section 3.3.2 (see Table 3.1). Studies have shown a good estimate for the capital share to be about 0.33 (see Acemoglu [13]). However, we follow Greiner et al. [4] who suggest $\alpha = 0.18$.

We then get a steady state for $T^* = 287.87$ and $M^* = 1.01$. So both values are lower

c^*	a^*	k^*	T^*	M^*	λ_1^*	λ_2^*	λ_3^*
0.2614	$4.2572\ 10^{-4}$	0.5314	287.8744	1.0092	3.825	$-5.5276\ 10^{-5}$	-0.0161

Table 3.3: Steady-state values for the modified problem, (3.20).

than in the model of the previous section. The per capita consumption of the steady state is $c^* = 0.26$, and the per capita capital is given by $k^* = 0.56$ in equilibrium. The per capita abatement spending in the long run is $a^* = 4.52\ 10^{-4}$. All steady-state values and the co-state variables are summed up in Table 3.3. The eigenvalues of the Jacobian are 6.4, 0.62, 0.21, -6.39, -0.61, and -0.2. Since three eigenvalues are negative, the steady state is saddle-point stable with a three-dimensional stable manifold. In Figure 3.4 we see the phase portrait for several initial values in the (k, T, M)-space. Different grey shades denote different initial values for M. For each initial point, the GHG concentration and the capital stay nearly constant until the temperature has reached a certain value. From then on, all trajectories with identical $M(0)$ and $k(0)$ and more-or-less arbitrary $T(0)$ converge almost along the same path to the optimum. It seems that the specific value of T mentioned above mainly depends on the corresponding initial value of the GHG concentration. In the following we perform a more detailed analysis of the behaviour of several trajectories, and we also examine the optimal choice of the control variables.

We analyse the time paths for three different initial points with fixed initial per capita capital $k(0) = 0.1$ and fixed initial temperature $T(0) = 289$. For the initial GHG concentration, $M(0)$, we assume values of 1 (which we will also call "low", which means a concentration of GHG at the pre-industrial level), 1.5 ("medium"), and 2 ("high"). In Figure 3.5 we see the paths for the state variables and in Figure 3.6 plots of the behaviour of the control variables are shown.

Conspicuously, the changes in capital and consumption do not depend on $M(0)$, as the time paths of all three initial points proceed more or less identically (Figure 3.5(a) and 3.6(a)). Both variables are at a low level in the beginning and converge in a concave way to the steady-state level.

In Figure 3.5(b) we see the paths of the temperature. The peaks for the medium and the high initial value respectively the trough for the low one, denote the specific values of T mentioned above. These values are 291.17 for the high trajectory, 289.71 for the medium, and 287.79 for the low time-path. Note, also for the higher initial values the paths temporarily drop under the long-run level, before they all converge from below to the steady-state level (Figure 3.5(b)).

The GHG concentration is the only state variable for which the trajectories start at different values. For the high and the medium starting point, the paths decline until they

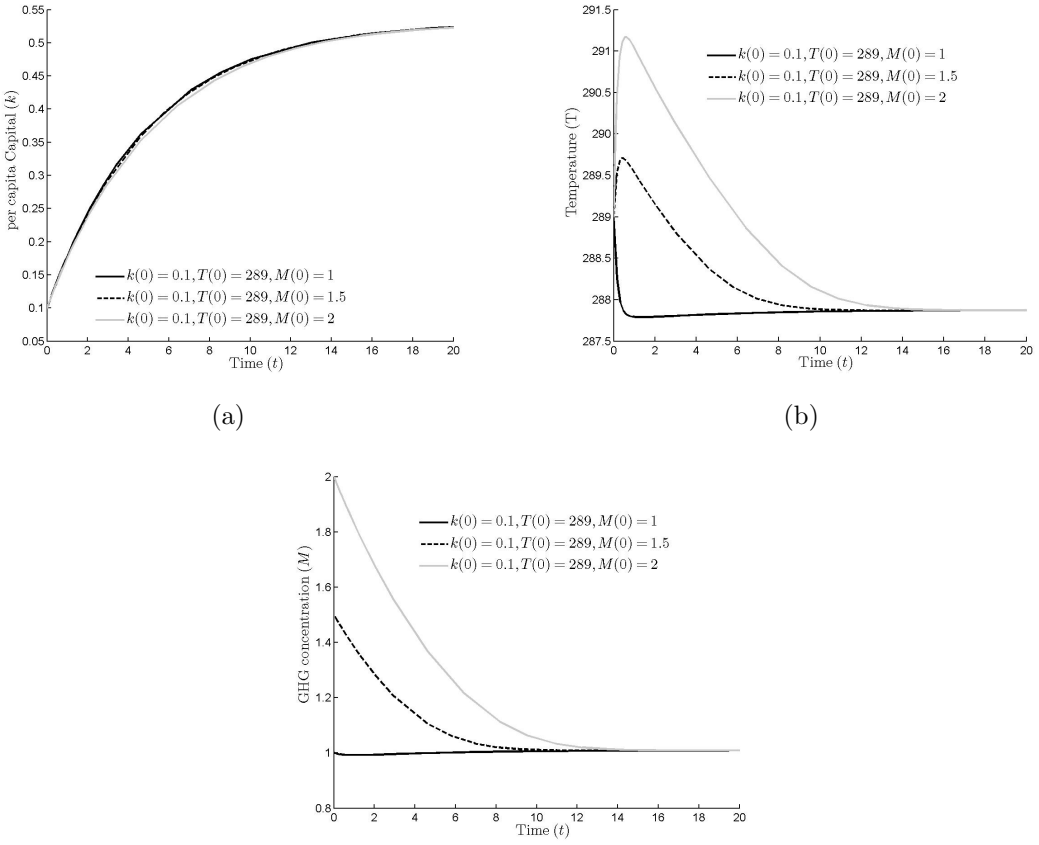

Figure 3.5: Time paths of the optimal state variables for three different initial points. The starting points differ only in the value of the GHG concentration.

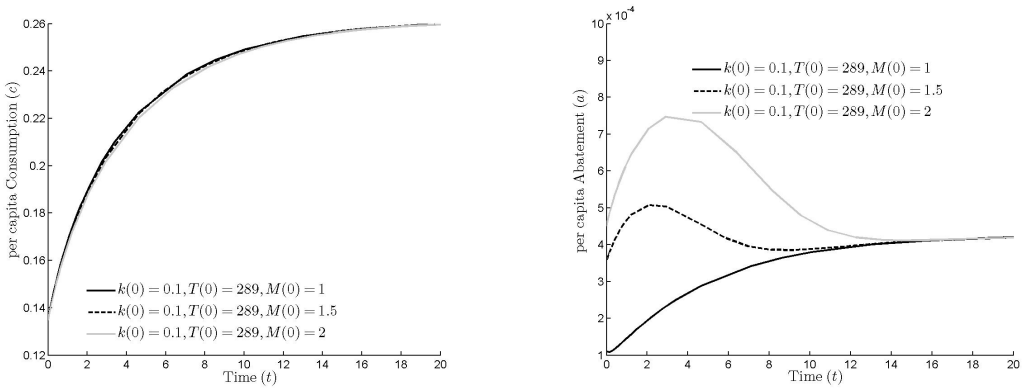

(a) (b)

Figure 3.6: Time paths of the optimal controls.

are under the long-run value and then converge to the steady state. The path for the low initial point always stays beneath the steady state. All three proceed in a convex way (Figure 3.5(c)).

In contrast to the consumption, the paths for abatement have different initial points for the different values of $M(0)$. The paths for the low and medium initial values start below the steady-state value, whereas the high one starts slightly above. The course of the optimal abatement spending can roughly be divided into two groups. For the two higher trajectories, the abatement levels first increase, and even the peak of the medium trajectory lies above its long-run level. Afterwards, both begin to fall until they are even under their steady-state level. On the other side, the lower trajectory even falls in the very short run but then monotonically converges to the steady state (Figure 3.6(b)).

3.4.3 Comparative Statics

In this section we discuss the influence of every single parameter and the robustness regarding the stability of the steady state w.r.t. changes of parameter values.

First, we claim that a steady state can only be realistic and hence admissible, if $T \geq T_{pre}$ and $M \geq M_{pre}$ hold, because it seems not a realistic scenario that optimal steady-state values lie under their pre-industrial level.

Because we are interested in the impact a change in a single parameter causes on the system, respectively the steady state, we investigate the percentual change of the control and state variables in comparison to the base case derived in the previous section (see Table 3.3). It is remarkable that all parameters have hardly any impact on the steady-state value of the temperature. The biggest changes for this variable occur by varying the parameters μ_1 and γ, which leads to a maximal bandwidth of $1.5 - 2\%$ off the base

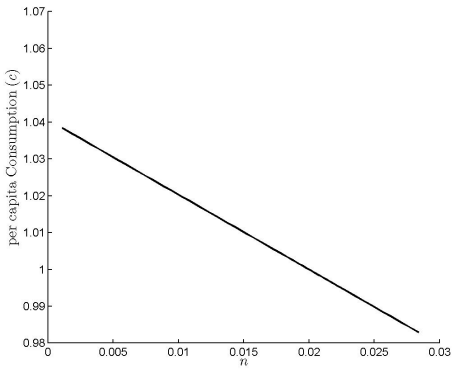

Figure 3.7: Comparative statics of c w.r.t. n.

steady state. All of the other parameters have far less impact.

We start the analysis of the parameter which has the lowest influence on all steady-state values, the heat-capacity, c_h. For the interval $(0, 1)$ we observe a maximum absolute deviation of less than 0.02% for each variable. So, effectively this parameter has no effect on the steady state.

Furthermore, β_1, which takes into account that a higher GHG concentration inhibits the warmth absorbtion of the oceans, has hardly any effect on c, k, and T. The effects concerning abatement and GHG concentration are less than 1% within the closed interval $[1, 2]$. But if we vary the base parameter value by only 1%, the steady-state values of M and a only change by about 0.02 percent. If we increase β_1, M shrinks and a grows, and vice versa if we lower the parameter.

The last parameter with similar characteristics is the labour growth rate, n. If we lower the base value of the growth rate by one percent, we can only observe a 0.04% raise in the per capita consumption. The opposite happens if we increase the parameter by the same percentage. If we investigate greater values (within the interval $(0, 0.03)$), such that the expression $(\rho - n)$ is positive (the base value of ρ is 0.03), the impact on c stays in the single-digit percentage range. With a growing n, we observe a linear decrease in c, see also Figure 3.7. The other values are barely affected.

Changes in the parameters a_1 and ψ have more or less the same effects. Both occur in the damage function describing the negative influence of a higher temperature on the output of the economy. For these two parameters we consider the range of $[0, 0.1]$. Hardly any changes in the values of c, k, and of course T occur. For the abatement and the GHG concentration, we observe a bigger impact, but we want to mention that an increase over the base case parameter value also has very low effects. The lower the parameter values, the lower a gets. On the other hand, M rises with a lower parameter value. Representatively, see Figure 3.8, where we show the comparative statics of a and

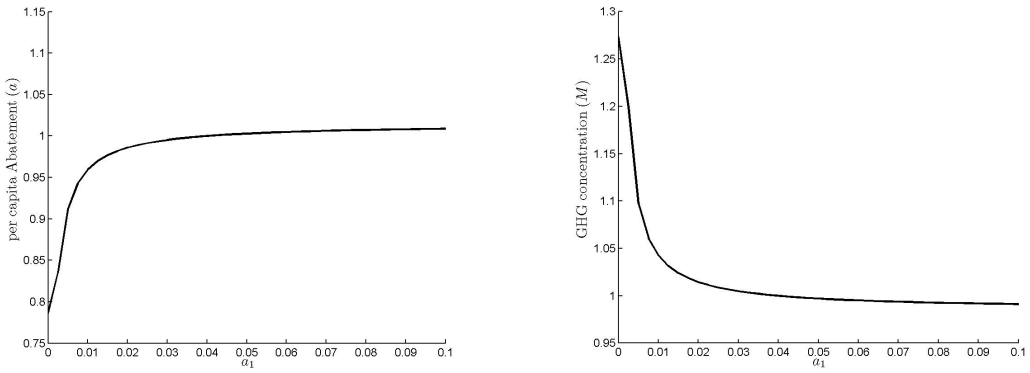

(a) (b)

Figure 3.8: Comparative statics of a and M for the parameter a_1. Note that these are qualitatively equivalent for ψ.

M as a function of a_1.

Next, we investigate the discount rate, ρ. The higher ρ, the lower the consumption, the abatement, and the capital. For a change of the parameter by 1 percent we get a deviation of 0.35% for a and k respectively 0.01% for c. The remaining two state variables stay pretty much constant. It is remarkable that a and k change quite similarly. This is also true for a greater deviation from the base case. The steady-state values for both are about 10% higher than the base case for ρ near the lower bound, 0.02, and then they decrease until they are about 46% beneath the primary level for $\rho = 0.1$.

A similar behaviour occurs if we investigate the depreciation rate, δ. Again, c, a, and k, but now also M decline with an increase of the parameter value. For example, the abatement and the capital steady-state values increase to about 4.5 times the base scenario if we set the depreciation rate equal to zero. For $\delta = 0.2$, the values of these two variables halve compared to the initial case. For detailed information on the comparative statics of δ see Figure 3.9.

For the parameter B we can distinguish between two groups. On the one hand, we observe an increase in c, a, and k w.r.t. B, and on the other hand, the temperature and the GHG concentration stay nearly constant. Figure 3.10(a) shows a plot for the consumption exemplarily for all raising variables, because all three behave similarly.

Next, we investigate ξ, which denotes the fraction of warmth absorbed by oceans. This parameter has hardly any influence on the steady-state values of the consumption, the capital, and the temperature. Greater impacts (which means $> 5\%$ drifts from the base steady state) on the abatement and the GHG concentration, a is a decreasing function and M is increasing, can only be observed for $\xi > 0.7$ which seems a quite unrealistic scenario. Lower values of ξ have hardly any influence on the steady state.

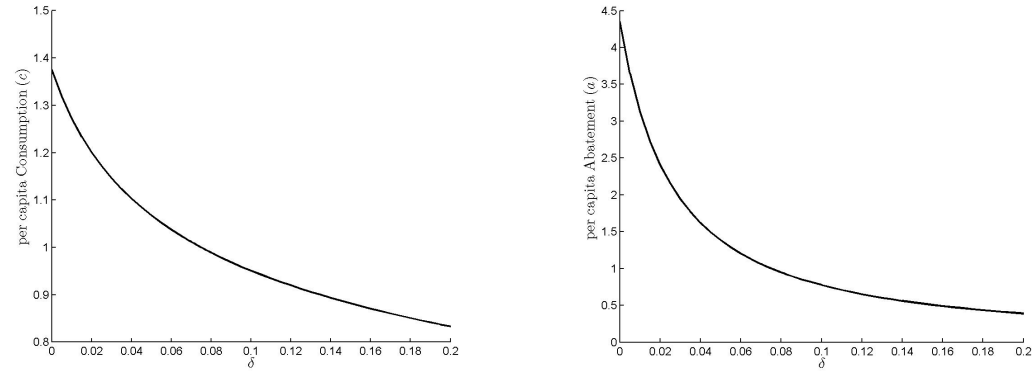

(a) (b)

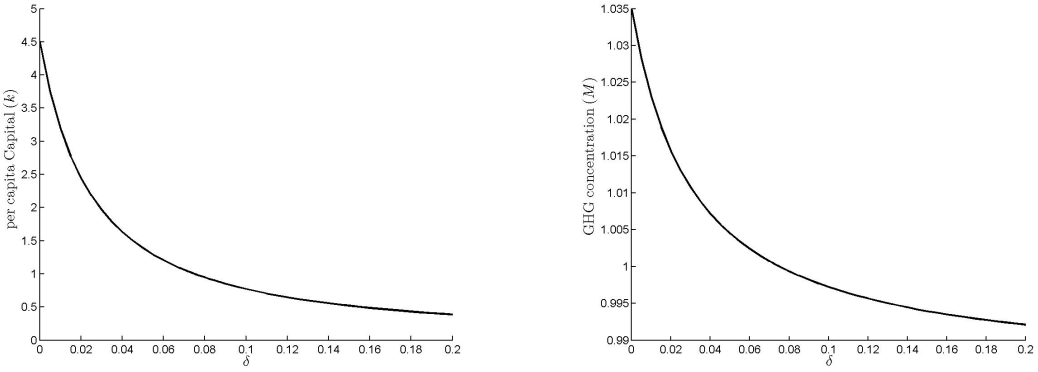

(c) (d)

Figure 3.9: Comparative statics for δ for all control and state variables except T.

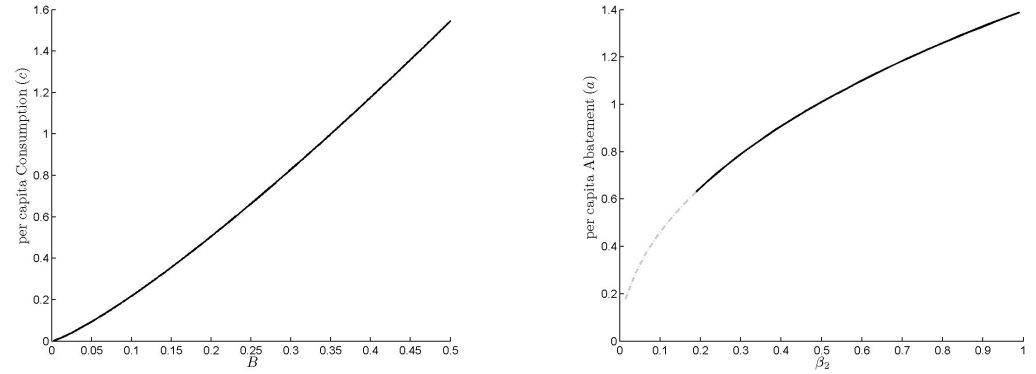

(a) Per capita consumption w.r.t. B. (b) Per capita abatement spending w.r.t. β_2.

Figure 3.10: Comparative statics for B and β_2.

A change in k_1, which is a constant in the albedo-function, shows analogous characteristics concerning the monotonicity. As above, c, k, and T are hardly influenced. Abatement spending decreases to 40% along with an increase of the parameter to $k_1 = 0.02$, and the GHG concentration increases to 2.5 times the base case value. If we lower the base parameter value by 2 percent, at least one of the restrictions, $T \geq T_{pre}$ and $M \geq M_{pre}$, is violated and the steady state is no longer realistic.

For the parameter, which takes into account that a part of emissions do not enter the atmosphere, β_2, only one variable, the per capita abatement, shows significant dependence. For the interval $(0, 1)$ we obtain that a has a range from below 20% to about 140% compared to the base case, but for $\beta_2 < 0.2$ the steady state is no longer admissible (see also Figure 3.10(b), in which the grey dash-dotted part denotes the unrealistic case). While c and T are barely affected, k and M still have a range of $\pm 1\%$ around the initial steady state. Note that the capital falls in β_2, while the GHG concentration grows.

More impact has the technology index, ε. Also here there exists a parameter range where the steady state gets unrealistic. This occurs if ε is below $8 \cdot 10^{-5}$. While the change in abatement spending is qualitatively equivalent to that of the parameter β_2, we now also observe a marginal influence on c. But a tenfold increase of the initial value of the parameter (which implies a more polluting technology) still lowers the value of c by only 1%. In that case, the per capita capital reduces by about 4% and the GHG concentration grows by 8%.

Next, we take a look at the inverse of CO_2 lifetime within the atmosphere, μ_1. The threshold for a realistic scenario for this parameter is at 0.26. For values of μ_1 below 0.26, the steady state is admissible. If we increase the base parameter value by 1%, also the optimal abatement-spending changes by about 1%, but in the opposite direction. All other variables effectively do not change. If we lower the parameter by the same amount, we observe the same effect as before, only vice versa. For sufficiently low parameter values we observe a major impact. While the per capita consumption and the capital fall, the abatement, the temperature, and the GHG concentration increase, see Figure 3.11.

The comparative statics of γ, a parameter to scale the emissions, show some interesting features. But first, let us start with the investigation of what happens if we vary the base value of the parameter by quite a small amount. If we increase the parameter to $\gamma = 1.01$, which means an increase of one percent, the optimal per capita consumption and the temperature do not change at all. The optimal choice of abatement declines by 1.22%, while per capita capital is only affected by a growth of about 0.01 percent. The GHG concentration decreases by 0.04%. If, on the other hand, we decrease the parameter by the same percentage, the effects occur vice versa, but with a slightly higher impact concerning a. In this case, the abatement spending increases by 1.26%. In general, the

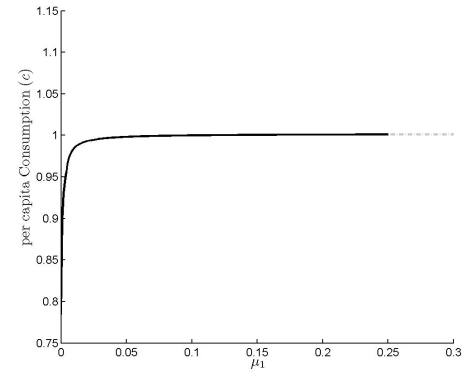

(a)

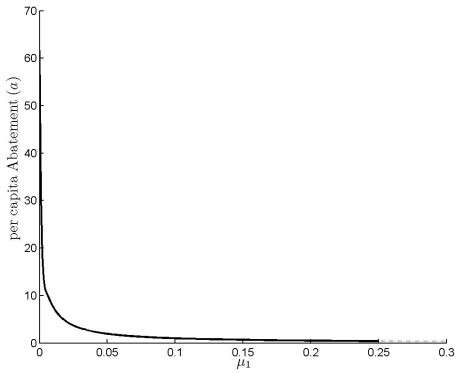

(b)

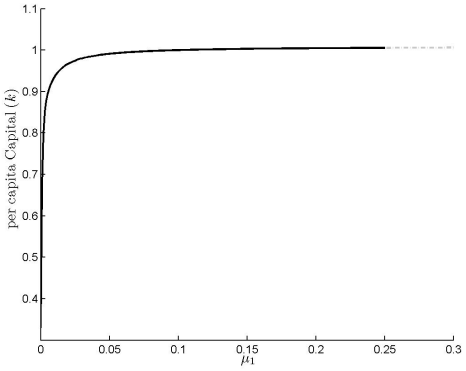

(c)

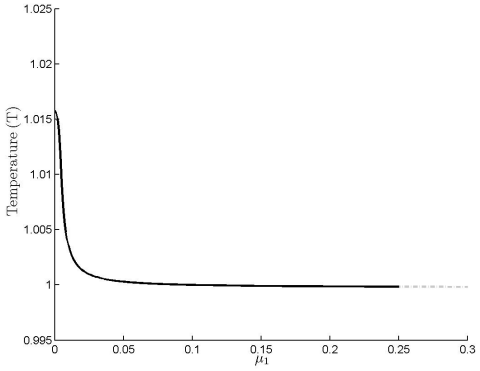

(d)

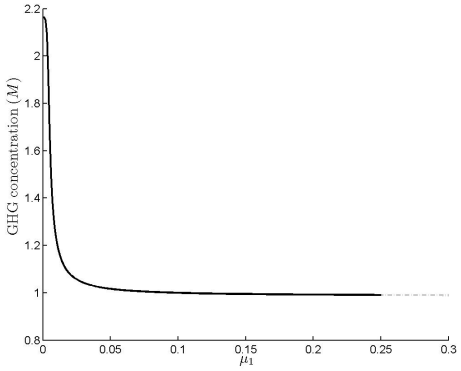

(e)

Figure 3.11: Comparative statics of μ_1 for all variables.

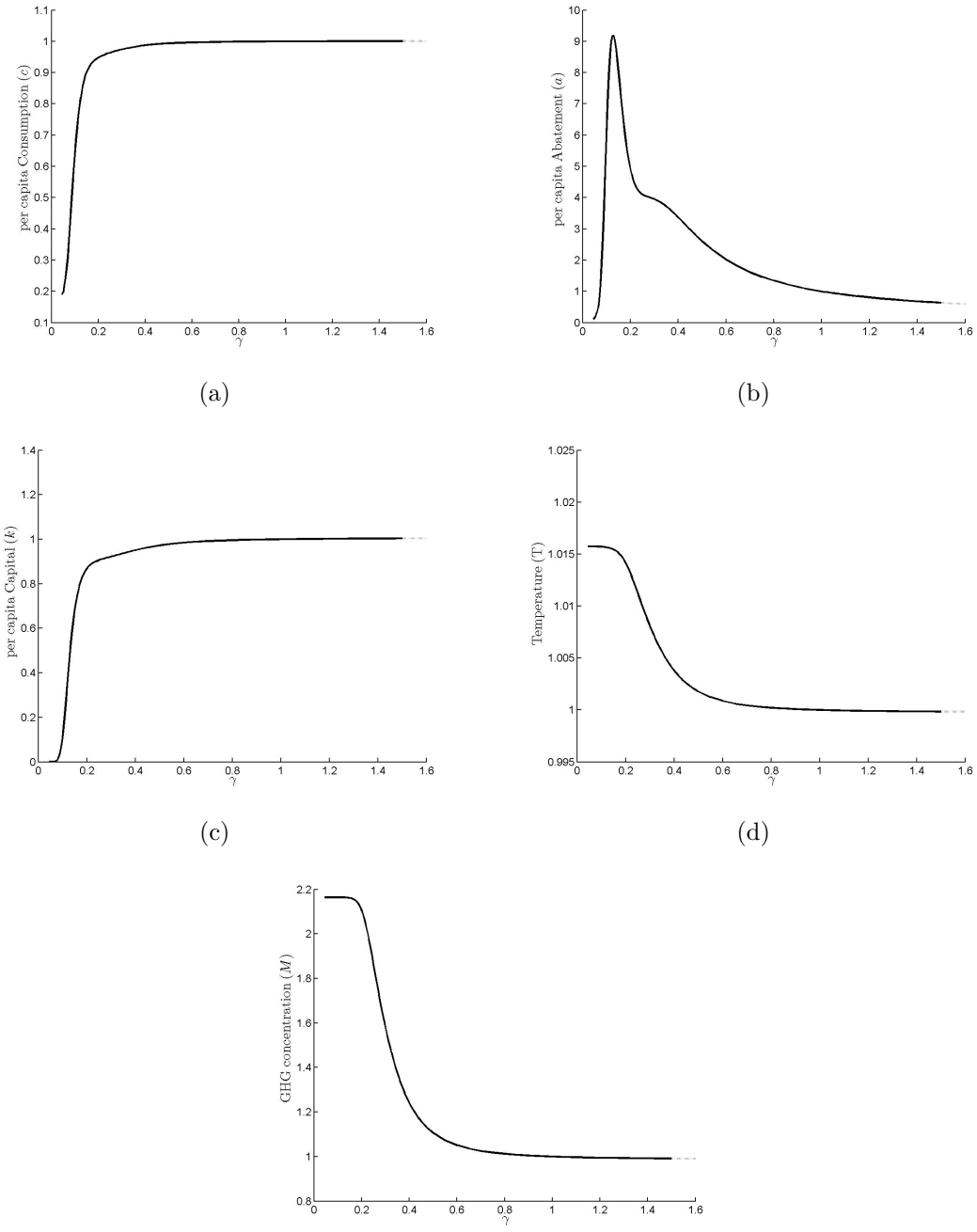

Figure 3.12: Comparative statics w.r.t. γ for all variables of the problem.

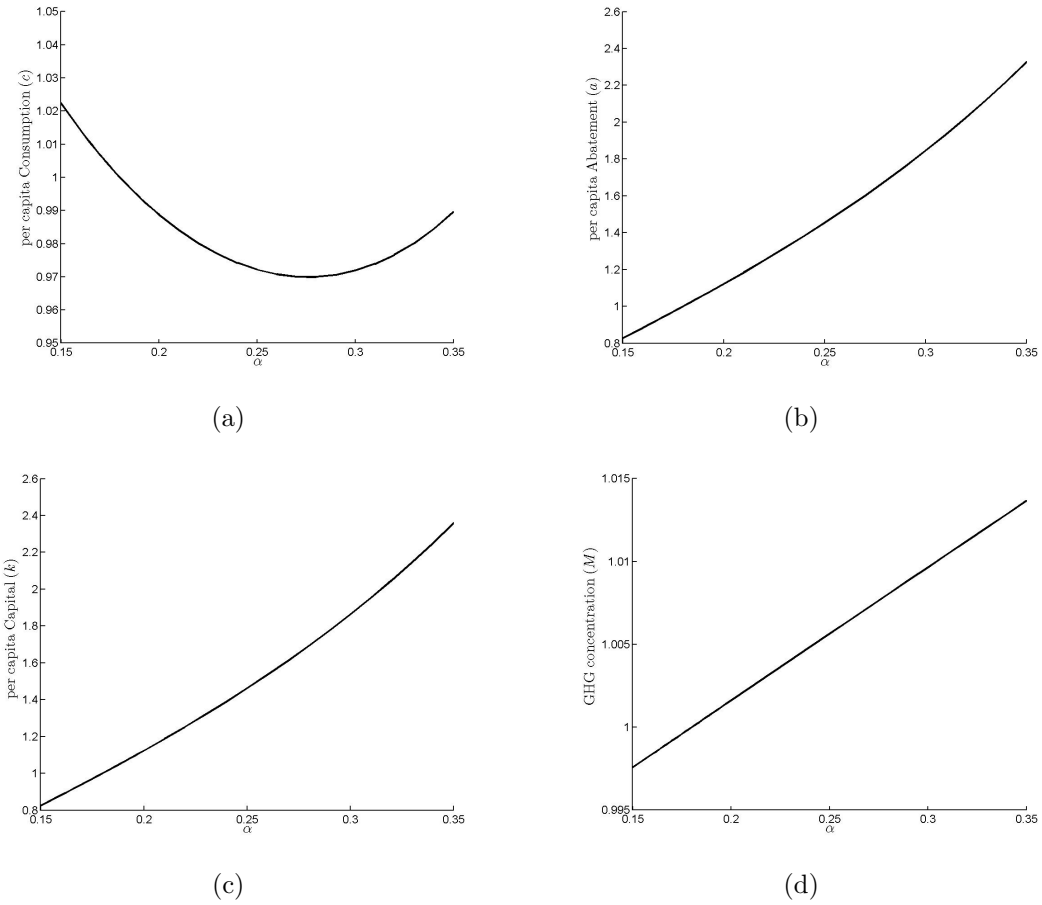

(a) (b) (c) (d)

Figure 3.13: Comparative statics w.r.t. α for the interval $[0.15, 0.35]$.

lower the parameter gets, the more extremely the variables change, except for a. There exists a threshold at a value of $\gamma = 0.125$ and an abatement-spending of 0.0039, which is more than ninefold of the base scenario. From this threshold, a decreases by further lowering the parameter. The plots for all five variables are shown in Figure 3.12. For values of γ greater than 1.5, the steady states becomes inadmissible.

For the parameter k_2, which occurs in the albedo function, some interesting results are obtained. While c, k, and T are barely affected if we lower the parameter value starting from the base case, the abatement together with the GHG concentration are highly influenced. If we lower the parameter by 0.01 respectively 5%, M doubles and a halves, and the effect gets even stronger for smaller values of k_2. If, on the other hand, we increase the parameter by only 0.1%, the GHG concentration falls under the threshold of $M = 1$, which we claimed as a necessary condition for a realistic and therefore an admissible steady state.

Finally, we analyse the sensitivity of the equilibrium w.r.t. to changes regarding the capital share, α. As mentioned above, studies showed that from empirical data we can

estimate α to be 0.33. However, Greiner et al. [4] decided to set $\alpha = 0.18$, which may take into account that the production function in this model does not consider labour force. Unfortunately, we have no further information, so we observe the changes of the steady state within the interval $[0.15, 0.35]$. Like all other parameters, also α has practically no influence on the long-run optimum of the temperature. Also the GHG concentration is barely affected. Compared to the base case, M is about 0.25% lower for $\alpha = 0.15$, while it increases by about 1.5 percent for $\alpha = 0.35$ (Figure 3.13(d)). Between these boundaries the dependence of M on α seems to be linear. A quite high impact can be observed concerning the steady-state values of abatement and capital. The decrease of the base parameter value of 0.18 to 0.15 implies a reduction of about 20% of both steady-state values. On the other hand, if we set the capital share equal to 0.32, both steady-state values are more than twice as much as in the base case (see Figures 3.13(b) and (c)). Contrary to the other variables, the per capita consumption does not behave monotonously within the underlying interval. At first it decreases due to higher parameter values, but after passing a threshold of about $\alpha = 0.28$, the steady-state value increases. Note, c does not increase enough within the chosen interval to reach the base case value again. It lies about one percent beneath it for $\alpha = 0.35$. For more details see also Figure 3.13(a).

Overview

For a better overview and also to make it easier to compare the impact of the variables, we sum up some information in Table 3.4. The upper line for each parameter shows the impact on the variables for an increase of the parameter by 1%, while the lower line shows the outcome for the decrease by the same percentage. The values presented in the table are given in terms of percent compared to the base case (see Table 3.3), and they are rounded to two decimals. The expression "-0" means that the effect is negative but less than 0.005%. Analogously, 0 implies an increase less than 0.005%, but not necessary really zero impact.

It is remarkable that only the parameters γ, α, and k_2 influence a couple of steady-state values by more than one percent. Most parameters have far less impact.

3.5 Conclusion

After these analyses we have a good understanding of the Greiner et al. model and its dynamics, especially for the problem with decreasing returns to scale. It is remarkable that the time paths of per capita capital and per capita consumption do not depend on the initial value of the GHG concentration. Further, it is interesting that for all initial

Parameter	c^*	a^*	k^*	T^*	M^*
ρ	-0.01	-0.34	-0.34	-0	-0
	0.01	0.35	0.35	0	0
n	-0.04	0	-0	-0	-0
	0.04	-0	0	0	0
B	0.7	0.7	0.7	0	0
	-0.7	-0.7	-0.7	0	0
a_1	-0	0.01	-0	-0	-0.01
	0	-0.01	0	0	0.01
ψ	-0	0.01	-0	-0	-0.01
	0	-0.01	0	0	0.01
δ	-0.17	-0.85	-0.86	-0	-0.01
	0.17	0.86	0.87	0	0.01
c_h	-0	-0	0	0	0
	-0	0	-0	-0	-0
β_1	-0	0.02	-0	-0	-0.02
	0	-0.02	0	0	0.02
ξ	0	-0.01	0	0	0.01
	-0	0.01	-0	-0	-0.01
β_2	-0	0.48	-0.01	0	0.01
	0	-0.48	0.01	-0	-0.01
μ_1	0	-0.97	0.01	-0	-0.02
	-0	0.98	-0.01	0	0.02
ϵ	-0	0.48	-0.01	0	0.01
	0	-0.48	0.01	-0	-0.01
γ	0	-1.2	0.01	-0	-0.04
	-0	1.3	-0.01	0	0.04
α	-0.11	1.1	1.1	0	0.01
	0.12	-1.1	-1.1	-0	-0.01
k_1	0	-0.35	0	-0	0.36
	-0	0.36	-0	0	-0.36
k_2	-0	1.5	-0.01	0	-1.5
	0	-1.5	0.01	-0	1.5

Table 3.4: Summary of comparative statics for the Greiner et al. [4] model with decreasing returns to scale.

conditions the temperature converges quickly to a certain level which mainly depends on the starting value of the GHG concentration. Another important conclusion is that small changes in most parameters do not very much affect the steady-state values.

Chapter 4

The Combined Model

The following chapter includes the main goal and corresponding results of this thesis. We combine the models presented in Chapter 2 and Section 3.4. For that purpose, we include Erickson's [5] idea of the quadratic term into the dynamics of the GHG concentration of the Greiner et al. [4] model. We are interested in the results of the new model and we will compare these to the ones obtained for the basic Greiner et al. model.

4.1 The Model

We consider the following formulation of the problem:

$$\max_{c,a} \int_{t=0}^{\infty} e^{-\rho t} L_0 e^{nt} \ln c \; dt, \tag{4.1a}$$

$$\text{s.t. } \dot{k} = B\, k^{\alpha}\, D_2(T) - c - a - (\delta + n)\, k, \tag{4.1b}$$

$$\dot{T}\, c_h = \frac{1367.5}{4}\,(1 - \alpha_1(T)) - \frac{1.131165}{1.09 \cdot 10^8}\, T^4 + \beta_1\,(1-\xi)\, 6.3\, \ln \frac{M}{M_{pre}}, \tag{4.1c}$$

$$\dot{M} = \beta_2 \left(\varepsilon \frac{k}{a}\right)^{\gamma} - [\mu_1 - \mu_2\,(T - T_{pre})]\; M, \tag{4.1d}$$

$$T(0) = T_0, M(0) = M_0, k(0) = k_0.$$

The model is very similar to the basic model given in (3.20). Indeed, the only difference is in the definition of the state dynamics of the GHG concentration (4.1d), in which we replaced the expression $\mu_1 M$ by the mixed-quadratic term $[\mu_1 - \mu_2\,(T - T_{pre})]\; M$. Again, a social planner maximises the discounted utility of consumption over an infinite time horizon.

4.1.1 Optimisation

As in the previous chapters we normalise L_0 and M_{pre} to unity and hence, the current-value Hamiltonian is given by

$$\begin{aligned} H(\cdot) = \ln c + \lambda_1 \left[B\, k^{\alpha}\, D_2(T) - c - a - (\delta + n)\, k\right] + \\ \lambda_2 \left[\frac{1367.5}{4}\left(1 - \alpha_1(T)\right) - \frac{1.131165}{1.09 \cdot 10^8}\, T^4 + \beta_1\,(1-\xi)\, 6.3\, \ln M\right] \frac{1}{c_h} + \\ \lambda_3 \left\{\beta_2 \left(\varepsilon\, \frac{k}{a}\right)^{\gamma} - \left[\mu_1 - \mu_2\,(T - T_{pre})\right]\, M\right\}. \end{aligned}$$

The necessary first-order conditions are then given by the equations (3.21a)-(3.21c) together with

$$\dot{\lambda}_2 = \lambda_2 \left[\rho - n + \frac{1}{c_h}\left(\frac{1367.5}{4}\alpha_1'(T) + \frac{4.52466}{1.09 \cdot 10^8} T^3\right)\right] - \lambda_1\, B\, k^{\alpha}\, D_2'(T) - \lambda_3\, \mu_2\, M$$

and

$$\dot{\lambda}_3 = \lambda_3 \left[\rho - n + \mu_1 - \mu_2\,(T - T_{pre})\right] - \lambda_2 \frac{\beta_1\,(1-\xi)\, 6.3}{c_h\, M}.$$

Like before, $D_2'(T)$ and $\alpha_1'(T)$ are given by (3.10) and (3.11), respectively. By using the first-order conditions we compute the following system of autonomous differential equations:

$$\begin{aligned} \dot{k} &= B\, k^{\alpha}\, D_2(T) - \frac{1}{\lambda_1} - \left[\frac{(-\lambda_3)\, \beta_2\, \gamma\, \varepsilon^{\gamma}\, k^{\gamma}}{\lambda_1}\right]^{\frac{1}{1+\gamma}} - (\delta + n)\, k, \\ \dot{T} &= \frac{1}{c_h}\left[\frac{1367.5}{4}\left(1 - \alpha_1(T)\right) - \frac{1.131165}{1.09 \cdot 10^8}\, T^4 + \beta_1\,(1-\xi)\, 6.3\, \ln M\right], \\ \dot{M} &= \beta_2^{\frac{1}{1+\gamma}} \left[\frac{\varepsilon\, k\, \lambda_1}{(-\lambda_3)\, \gamma}\right]^{\frac{\gamma}{1+\gamma}} - \left[\mu_1 - \mu_2\,(T - T_{pre})\right]\, M, \\ \dot{\lambda}_1 &= \lambda_1 \left[\rho + \delta - \alpha\, B\, k^{\alpha-1}\, D_2(T)\right] + \left[\frac{(-\lambda_3)\, \beta_2\, \gamma\, \varepsilon^{\gamma}\, \lambda_1^{\gamma}}{k}\right]^{\frac{1}{1+\gamma}}, \\ \dot{\lambda}_2 &= \lambda_2 \left[\rho - n + \frac{1}{c_h}\left(\frac{1367.5}{4}\alpha_1'(T) + \frac{4.52466}{1.09 \cdot 10^8} T^3\right)\right] - \lambda_1\, B\, k^{\alpha}\, D_2'(T) - \lambda_3\, \mu_2\, M, \\ \dot{\lambda}_3 &= \lambda_3 \left[\rho - n + \mu_1 - \mu_2\,(T - T_{pre})\right] - \lambda_2 \frac{\beta_1\,(1-\xi)\, 6.3}{c_h\, M}. \end{aligned}$$

Then a steady state is given as the solution of the system $\dot{k} = \dot{T} = \dot{M} = \dot{\lambda}_1 = \dot{\lambda}_2 = \dot{\lambda}_3 = 0$.

c^*	a^*	k^*	T^*	M^*	λ_1^*	λ_2^*	λ_3^*
0.2614	$4.263\ 10^{-4}$	0.5314	287.8711	1.0085	3.825	$-5.5355\ 10^{-5}$	-0.0162

Table 4.1: Steady-state values (control, state, and co-state variables) for the combined model, (4.1).

4.1.2 Numerical Analysis

If we solve the system $\dot{k} = \dot{T} = \dot{M} = \dot{\lambda}_1 = \dot{\lambda}_2 = \dot{\lambda}_3 = 0$ with the same parameter set as used in the previous chapter (see Table 3.1 and $\alpha = 0.18$), together with the new parameter value $\mu_2 = 0.001$ (see Chapter 2), we get one solution by using `OCMat`. Of course, we can only search for steady states within a certain range. For the per capita capital, we chose a range of $[0, 50]$. For the temperature we searched within $[287, 315]$, because 287 is already under the pre-industrial level, and 315 K means a temperature increase of about 27 K. Compared to the goal, set by the United Nations Framework Convention on Climate Change (UNFCCC) [14], to limit the temperature increase to 2 K, our bandwidth seems big enough. Last, for the GHG concentration we considered the interval $[1, 30]$, which means a value between the pre-industrial level and the 30-fold of it.

The steady state per capita consumption is about 0.26, and the second control variable, per capita abatement spending, is $4.26 \cdot 10^{-4}$. The long-run average temperature raises to the level of 287.87 K, which means an increase of 0.07 K respectively 0.07 °C compared to the pre-industrial level. The steady-state value of the GHG concentration lies about 0.9% over the pre-industrial level (which we normalised to unity). Last, per capita capital is about 0.53.

All these values together with the co-state variables are summed up in Table 4.1. The eigenvalues of the Jacobian evaluated at this steady state are 6.41, 0.62, 0.21, -6.4, -0.61, and -0.2. Therefore, the equilibrium is saddle-point stable.

The phase portrait of the model is given in Figure 4.1. Note, we used the same initial points for the trajectories as for the phase portrait of the Greiner et al. model with decreasing returns to scale. For the black arcs we pick $M(0) = 1$, for the light grey curves the initial value of the GHG concentration is 1.5, and for the dark grey ones we set $M(0) = 2$.

What is striking is the fact that the extension of the problem has hardly any effect on the steady state of the system (compare Table 3.3). Furthermore, the phase portrait of the combined model looks more or less like the one of Greiner et al.'s model (see Figure 3.4). The same applies to the time paths.

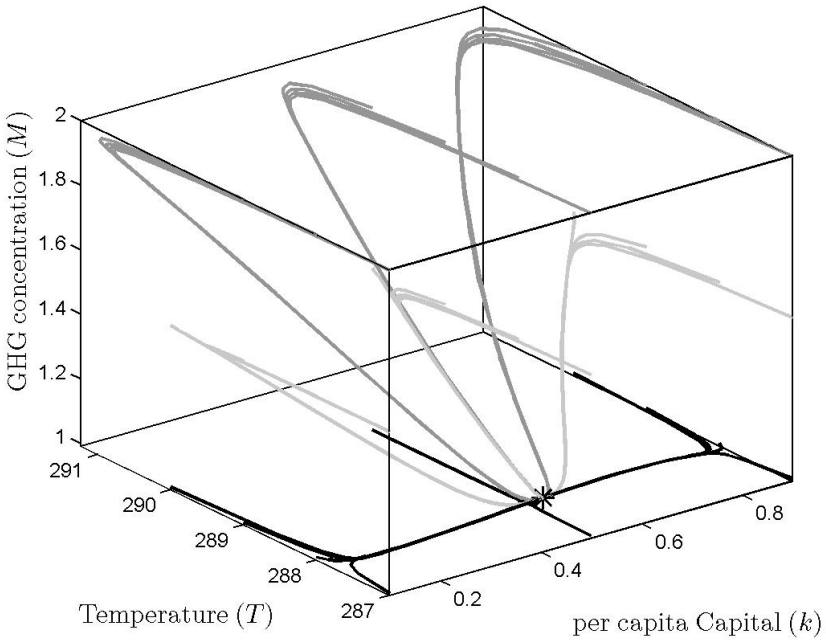

Figure 4.1: Phase portrait of the model (4.1) in the (k, T, M)-space.

4.1.3 Comparative Statics

In this section we want to analyse the influence of the newly implemented parameter μ_2. Before we start, we claim again that a steady state can only be realistic if $T \geq T_{pre}$ and $M \geq M_{pre}$ hold (analogously to the previous chapter).

The plots we present show a range for the parameter μ_2 from zero to 0.1, which means that the right side of the investigated interval is 100 times bigger than the original estimate. In Figure 4.2 we see that per capita consumption and per capita capital first decrease and then grow, while per capita abatement behaves vice versa. The temperature as well as the GHG concentration fall monotonically. The dash-dotted grey parts of the curves denote the area for which at least one of the assumptions $T \geq T_{pre}$ and $M \geq M_{pre}$ is violated. This occurs if μ_2 is greater than 0.014. Note, the vertical axes do not show absolute values, but rather show values relative to the steady-state values for $\mu_2 = 0$. This shows relative changes compared to Greiner et al.'s model with decreasing returns to scale. We see that these changes are rather small. The biggest shift can be observed for the abatement and the GHG concentration. If we only study the range of the parameter, which leads to a realistic steady state, μ_2 only has an effect of less than 2 percent at maximum. On the other variables, the new parameter has even less influence (in the order of 10^{-2} percent and less).

We are also interested in the value of the complete new term. In Figure 4.3, the value

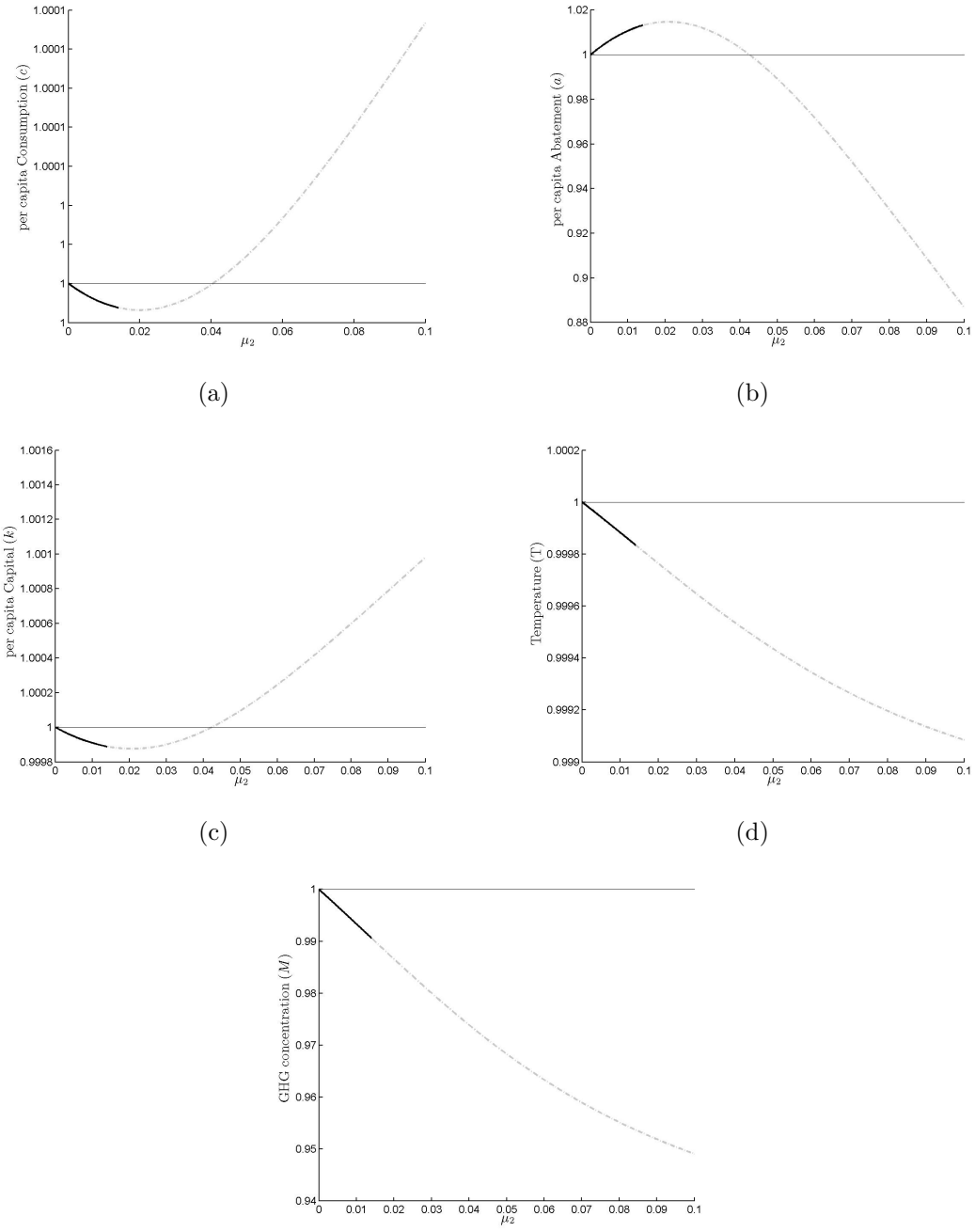

Figure 4.2: Comparative statics for the parameter μ_2.

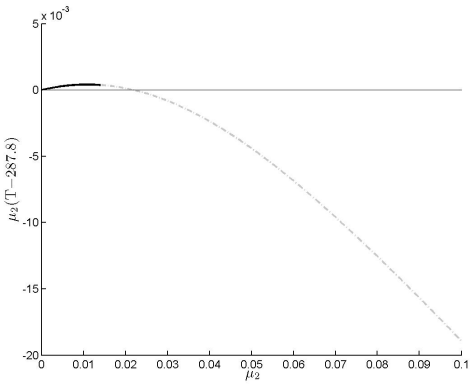

Figure 4.3: Value of the new term, $\mu_2 (T - T_{pre})$.

of $\mu_2 (T - T_{pre})$ is shown. Also here, the dash-dotted part of the curve denotes the range where the steady state becomes non-admissible in the sense described above. For values of μ_2 where the steady state has realistic values, the expression is positive but very small in relation to μ_1, which is $= 0.1$. This fact obviously is responsible for the similarity of the two models.

Chapter 5

Summary and Conclusion

The goal of this thesis was to analyse the impact of the implementation of an innovative aspect in a rather simple optimal control model of global warming into a well-established economic growth model with global warming. For that purpose, we implemented the idea of Erickson [5] that the dynamics of the GHG concentration in our atmosphere depend negatively on increasing surface temperature into a well-known model by Greiner et al. [4].

First, we will shortly sum up the results of the previous chapters.

5.1 Summary

We started with the introduction of a model by Gary M. Erickson [5]. We began analysing his model by assuming the original control variable as exogenously given. As a result, we found that, depending on this variable, the system has either two, one or zero steady states. For this simple model, it was also possible to verify the existence of a so-called *blue sky* bifurcation analytically. Afterwards, we took a deeper look at the original model. We worked out that the problem yields zero to two steady states depending on the parameters used in the model. Furthermore, by using a specific set of parameter values, we derived the corresponding phase portrait of the problem and optimal time paths for different initial values. Moreover, as such parameters are only estimates and they are probably not exact, we performed sensitivity and bifurcation analyses for all model parameters. Except for the time preference rate, r, we obtained two steady states for all other parameters. However, only one was admissible and stable at the same time. Regarding r, we found the typical *blue sky* bifurcation. Again only one steady state was stable and admissible.

Crucial influence was shown regarding the *quadratic* parameter, which we later implemented into the growth model. We showed that without this part of the dynamics the problem simplifies and hence only has one unique, saddle-point-stable steady state.

Next, we introduced an energy balance model to describe the atmosphere as well as the interaction between the average surface temperature and the GHG concentration as suggested in Greiner et al. [4]. The first approach was to model an economy with constant returns to scale. It was possible to reduce the canonical system to one equation with one variable, but due to the complexity of the problem we were not able to solve the corresponding system analytically. So, we specified a set of parameters and solved the resulting model numerically. We found one unique steady state within a realistic interval of earth's surface temperature, which was again saddle-point stable. Afterwards, we implemented a production function with decreasing returns to scale and solved the problem with the same parameter set again numerically. By using the `Matlab` toolbox `OCMat` we found one saddle-point equilibrium. It was remarkable that the steady-state values regarding the surface temperature and the GHG concentration did not vary much from their pre-industrial levels. After we looked at some optimal time paths for three different sets of initial values, we concluded the chapter with the comparative statics for the parameters of the model.

In Chapter 4 we introduced the idea of Erickson [5] into the Greiner et al. [4] model with decreasing returns to scale. Hence, a new parameter entered the system. Again, we derived the canonical system and solved it numerically by using the toolbox `OCMat`. Finally, we carried out some sensitivity analysis for the new parameter. We showed that only for sufficiently small values, the steady state is admissible.

5.2 Conclusion

First, we want to point out that for the three models discussed in Chapters 3 and 4, the steady-state values are pretty close to the pre-industrial level regarding the surface temperature and the GHG concentration. The more complicated the models become (from constant to decreasing returns to scale and finally the combined model in Chapter 4), the closer the steady state is at pre-industrial level. The long-run optimal GHG concentration of the atmosphere lied only 2% above the pre-industrial level for the first model and decreased to be only one percent above this level for the other two models. The equilibrium temperature increase for all models was about 0.1 °C or less.

From the comparative statics in Chapter 3 we can state that all parameters hardly affect the steady-state value of the average surface temperature of earth. Further, it is remarkable that based on this analysis, the heat capacity of earth has no influence on the equilibrium at all.

The core statement of this thesis follows from Chapter 4. It seems that the implemen-

tation of the new term has hardly any impact on the outcome of the model. Compared to the Greiner et al. model with decreasing returns to scale, the equilibrium does not differ before the third decimal place regarding the temperature, while the absolute differences of the other variables are even smaller. Moreover, the phase portrait and the time paths look similar and are qualitatively the same. This may be accounted to the relatively low value of the new implemented term, which is at most of the order 10^{-3}.

Concluding, from our point of view it has no advantage to implement this new term. For the parameter values we assumed, the effect is obviously very small. As a consequence, the qualitative behaviour of the dynamics of the model is not influenced. Moreover, higher complexity implies higher CPU usage while solving and analysing the problem numerically.

Appendix A

Proofs of Chapter 2

A.1 Proof of Proposition 2.1

Proof. Setting $\dot{G} = \dot{T} = 0$ yields a system with two solutions given by

$$G^*_{1,2} = \frac{\beta}{2\,\gamma\,\varepsilon} \pm \sqrt{\frac{\beta^2}{4\,\gamma^2\,\varepsilon^2} - \frac{m}{\gamma\,\varepsilon}} \text{ and}$$
$$T^*_{1,2} = \frac{\beta}{2\,\gamma} \pm \sqrt{\frac{\beta^2}{4\,\gamma^2} - \frac{m\,\varepsilon}{\gamma}}.$$

If the expression under the square root, $\frac{\beta^2}{4\,\gamma^2\,\varepsilon^2} - \frac{m}{\gamma\,\varepsilon}$, is greater (equal,lower) zero, the problem has two (one,zero) real roots. If we then isolate m, we directly get the statements of the proposition. ■

A.2 Proof of Proposition 2.2

Proof. Setting $\dot{G}$, $\dot{T}$, $\dot{\mu}_1$, and $\dot{\mu}_2$, given by (2.1), (2.2), (2.8), and (2.9), equal to zero and using (2.7), we can derive the following equation:

$$a\,[(r+\beta)(r+\delta) - \gamma\varepsilon(r+2\delta)G] = b\delta\varepsilon(\beta - \gamma\varepsilon G)G.$$

Now we define $f(G) := a\,[(r+\beta)(r+\delta) - \gamma\varepsilon(r+2\delta)G]$ and $h(G) := b\delta\varepsilon(\beta - \gamma\varepsilon G)G$. Then f is a linear and decreasing function of G and $f(0) = a(r+\beta)(r+\delta) > 0$. On the other hand, h is concave, has its peak value at $G_{max} = \frac{\beta}{2\gamma\varepsilon} > 0$, and $h(0) = 0$. So, if $f(G_{max}) < h(G_{max})$ holds, the two functions intersect twice and thus the problem yields two steady states.

Inserting $G_{max} = \frac{\beta}{2\gamma\varepsilon}$ in the inequality $f(G_{max}) < h(G_{max})$ and solving this inequality for r, keeping in mind that $r > 0$ must hold by the definition of the problem, we can

derive the condition $r < \frac{1}{4}\left(\sqrt{(\beta+2\delta)^2 + \frac{4b\beta^2\delta}{a\gamma}} - (\beta+2\delta)\right)$. ■

A.3 Proof of Proposition 2.3

Proof. We have to show, that $\beta - \gamma T^* > 0$ holds for the lower steady state.

$$G_l^* = \frac{1}{2\gamma\varepsilon}\left\{\frac{a\gamma(r+2\delta)}{b\delta} + \beta - \sqrt{\left[\beta + \frac{a\gamma(r+2\delta)}{b\delta}\right]^2 - \frac{4a\gamma(r+\beta)(r+\delta)}{b\delta}}\right\}$$

together with the relation $\varepsilon G_l^* = T_l^*$ yields

$$\beta - \gamma T_l^* = \beta - \frac{\gamma\varepsilon}{2\gamma\varepsilon}\left\{\frac{a\gamma(r+2\delta)}{b\delta} + \beta - \sqrt{\left[\beta + \frac{a\gamma(r+2\delta)}{b\delta}\right]^2 - \frac{4a\gamma(r+\beta)(r+\delta)}{b\delta}}\right\},$$

or equivalently

$$\beta - \gamma T_l^* = \frac{1}{2}\left\{\beta - \frac{a\gamma(r+2\delta)}{b\delta} + \sqrt{\left[\beta + \frac{a\gamma(r+2\delta)}{b\delta}\right]^2 - \frac{4a\gamma(r+\beta)(r+\delta)}{b\delta}}\right\}.$$

A sufficient condition for the last expression to be positive is $\beta - \frac{a\gamma(r+2\delta)}{b\delta} > 0$, which also can be rewritten as $r < \frac{b\beta\delta}{a\gamma} - 2\delta$. ■

A.4 Proof of Proposition 2.4

Proof. From the FOC we can derive the following system of differential equations:

$$\begin{aligned}
\dot{G} &= -\beta G - \frac{a}{\mu_1}, \\
\dot{T} &= \delta(\varepsilon G - T), \\
\dot{\mu}_1 &= \mu_1(r+\beta) - \mu_2\delta\varepsilon, \\
\dot{\mu}_2 &= \mu_2(r+\delta) + b.
\end{aligned}$$

Solving $\dot{G} = \dot{T} = \dot{\mu}_1 = \dot{\mu}_2 = 0$ directly leads to the steady-state values given in (2.15). To investigate stability we derive the Jacobian at the steady state,

$$J(G^*, T^*, \mu_1^*, \mu_2^*) = \begin{pmatrix} -\beta & 0 & a\left[\frac{(r+\beta)(r+\delta)}{b\delta\varepsilon}\right]^2 & 0 \\ \delta\varepsilon & -\delta & 0 & 0 \\ 0 & 0 & r+\beta & -\delta\varepsilon \\ 0 & 0 & 0 & r+\delta \end{pmatrix}.$$

It is easy to see that the eigenvalues of J are $\lambda_1 = -\beta$, $\lambda_2 = -\delta$, $\lambda_3 = r + \beta$, and $\lambda_4 = r + \delta$, so two are positive and two are negative. ■

A.5 Proof of Proposition 2.5

Proof. $g(r)$ is defined as the discriminant of the right side of Equation (2.10). So we have to investigate the sign of g depending on the parameters. At first we rewrite it to

$$g(r) = r^2\left[\frac{a\gamma}{b\delta}\left(\frac{a\gamma}{b\delta} - 4\right)\right] + r\left[4\frac{a\gamma}{b\delta}\left(\frac{a\gamma}{b} - \frac{\beta}{2} - \delta\right)\right] + \beta^2 + 4\left(\frac{a\gamma}{b}\right)^2.$$

So, g is a quadratic function w.r.t. r with $g(0) > 0$ and zeros

$$r_{1,2} = \frac{2\left(\frac{\beta}{2} + \delta - \frac{a\gamma}{b}\right) \pm \sqrt{4\left(\frac{\beta}{2} + \delta - \frac{a\gamma}{b}\right)^2 - \left(\frac{a\gamma}{b\delta} - 4\right)\left(\frac{\beta^2 b\delta}{a\gamma} + 4\frac{a\gamma\delta}{b}\right)}}{\frac{a\gamma}{b\delta} - 4}.$$

For the claims of the proposition we then get

1. As $\frac{a\gamma}{b\delta} - 4 < 0$ holds, the function g is concave. Together with $g(0) > 0$, we get one negative (r_1) and one positive (r_2) zero. Furthermore, g is greater zero for $r \in (0, r_2)$.

2a. In that case, $g(r)$ is convex and we already know $g(0) > 0$. We assume that r_1 and r_2 do not exist, so g is positive for all values of r, because it can not intersect the $g(r) = 0$ axis. If, on the other hand, $\frac{\beta}{2} + \delta - \frac{a\gamma}{b} < 0$ holds, both zeros are negative and so g is positive for all positive r.

2b. As above, $g(r)$ is convex and again $g(0) > 0$ holds. $\frac{\beta}{2} + \delta - \frac{a\gamma}{b} > 0$ guarantees that both zeros are positive. This directly leads to the proposition.

3. As $\frac{a\gamma}{b\delta} - 4 = 0$ holds, g simplifies to a linear function: $g(r) = 16r\left(3\delta - \frac{\beta}{2}\right) + \beta^2 + 64\delta^2$. As in (3a) g is increasing in r and $g(0) > 0$ holds, g is positive for all $r > 0$. In

(3b) it is monotonically decreasing and also $g(0) > 0$ holds. As g has one zero at $r = \frac{\beta^2+64\delta^2}{8(\beta-6\delta)}$, g is positive for the interval given in (3b).

■

A.6 Proof of Proposition 2.6

Proof. Starting with equation (2.11), we can also transform this equation to $k(\gamma)$ as defined in Proposition 2.6. So we have to investigate its sign. At first we look at the zeros of (2.16), respectively under which condition they exist or not. Let us define $p := -\frac{2br\delta[2(r+\delta)+\beta]}{a(r+2\delta)^2}$ and $q := \left[\frac{b\beta\delta}{a(r+2\delta)}\right]^2$. Then k has one zero, if $\left(\frac{p}{2}\right)^2 - q = 0$ holds. Applying p and q as defined before and solving it w.r.t. r we get two solutions, where one of them is negative. As we assumed positive values for all parameters, there remains one (positive) value

$$r = -\frac{\delta}{2} + \sqrt{\left(\frac{\delta}{2}\right)^2 + \beta\delta}.$$

1. As k is convex and positive at $\gamma = 0$, we get, that it has one zero at $\gamma = \frac{br\delta[2(r+\delta)+\beta]}{a(r+2\delta)^2}$ and is positive otherwise.

2. If $r < -\frac{\delta}{2} + \sqrt{\left(\frac{\delta}{2}\right)^2 + \beta\delta}$ holds, $k(\gamma)$ has no zeros, which directly leads to the proposition.

3. The function (2.16) has two zeros if $r > -\frac{\delta}{2} + \sqrt{\left(\frac{\delta}{2}\right)^2 + \beta\delta}$ holds. It is easy to see that they are both positive (keep in mind, that p is negative for all parameter combinations). Together with the characteristics mentioned above, this leads to the proposition.

■

Appendix B

Appendix to Chapter 3

B.1 Greiner et al. Model: Function $\dot{\lambda}_2$

Proposition B.1. *For $\dot{\lambda}_2$ given in (3.19), $\lim_{T\to\infty} \dot{\lambda}_2 = 0$ holds.*

Proof. We start with the definition of $\dot{\lambda}_2$ given in (3.19). This implies

$$\begin{aligned}\lim_{T\to\infty} \dot{\lambda}_2 = \lim_{T\to\infty} \Bigg\{ & -\frac{(\omega_1+\mu_1)\,\varepsilon\,c_h}{\gamma\,\omega_1\,\omega_2}\left[\frac{\mu_1^{1+\gamma}}{\beta_2}\exp\left(\frac{\omega_4\,T^4-\omega_3\,(1-\alpha_1(T))}{\omega_2}\right)\right]^{-\frac{1}{\gamma}}\cdot \\ & \left(\omega_1+\frac{\omega_3\,\alpha_1'(T)+4\,\omega_4\,T^3}{c_h}\right)-\frac{B\,D_2'(T)}{\omega_1}\Bigg\} = \\ = \underbrace{-\frac{(\omega_1+\mu_1)\,\varepsilon\,c_h}{\gamma\,\omega_1\,\omega_2}\mu_1^{-\frac{1+\gamma}{\gamma}}\beta_2^{\frac{1}{\gamma}}}_{=:U} & \lim_{T\to\infty} \underbrace{\frac{\omega_1+\frac{\omega_3\,\alpha_1'(T)+4\,\omega_4\,T^3}{c_h}}{\exp\left(\frac{\omega_4\,T^4-\omega_3(1-\alpha_1(T))}{\omega_2}\right)^{\frac{1}{\gamma}}}}_{=:V} - \lim_{T\to\infty}\underbrace{\frac{B\,D_2'(T)}{\omega_1}}_{=:W}.\end{aligned}$$

U: This expression only contains parameters with positive values. Therefore, U is a strict negative constant.

V: $\lim_{T\to\infty} V$ is of the form $\frac{\infty}{\infty}$. To see this, we first investigate the numerator. The important parts are $\alpha_1'(T)$ and T^3, where $\alpha_1'(T) = -\frac{k_1}{1+\frac{\pi^2}{4}(T-293)^2}$ converges to zero and T^3 to infinity for $T\to\infty$. Therefore, $\omega_1 + \frac{\omega_3\,\alpha_1'(T)+4\,\omega_4\,T^3}{c_h}$ converges to ∞. Second, the term $(1-\alpha_1(T)) = k_1\frac{2}{\pi}\arctan\left(\frac{\pi(T-293)}{2}\right)+k_2$ converges to k_1+k_2, because $\lim_{T\to\infty}\arctan(\cdot)=\frac{\pi}{2}$ holds, and as $\lim_{T\to\infty} T^4=\infty$, this implies $\lim_{T\to\infty}\exp(\cdot)=\infty$. If we then apply L'Hôspital's rule, we get, that $\lim_{T\to\infty} V = 0$ is true.

W: The only part which depends on T is $D_2'(T)$. If we now apply L'Hôspital's rule on $\lim_{T\to\infty} D_2'(T) = -2\psi\lim_{T\to\infty}\frac{a_1\,(T-287.8)}{[a_1\,(T-287.8)^2+1]^{1+\psi}}$ we get $\lim_{T\to\infty} W = 0$.

By combining all three parts we get the proposition. ■

References

[1] IPCC. *Climate Change 2013: The Physical Science Basis - Summary for Policymakers*. Website, 2013. http://www.climatechange2013.org/images/uploads/WGIAR5-SPM_Approved27Sep2013.pdf (last accessed on 29 October 2013).

[2] Pachauri R.K., Reisinger A. (eds.). *Climate Change 2007: Synthesis Report*. IPCC, Geneva, Switzerland, 2007.

[3] Greiner A., Semmler W. Economic growth and global warming: A model of multiple equilibria and thresholds. *Journal of Economic Behavior & Organization*, 57(4):430–447, 2005.

[4] Greiner A., Grüne L., Semmler W. *Growth and Climate Change: Threshold and Multiple Equilibria*. SCEPA Working Papers 2009-7, Schwartz Center for Economic Policy Analysis (SCEPA), The New School, March 2009.

[5] Erickson G.M. *Optimal Control of Global Warming*. Website, December 2012. http://ssrn.com/abstract=2193945 (last accessed on 29 October 2013).

[6] Feichtinger G., Hartl R.F. *Optimale Kontrolle ökonomischer Prozesse: Anwendungen des Maximumprinzips in den Wirtschaftswissenschaften*. Walter de Gruyter, Berlin, 1986.

[7] Nordhaus W.D. To slow or not to slow: The economics of the greenhouse effect. *The Economic Journal*, 101:920–937, 1991.

[8] Cox P.M., Betts R.A., Jones C.D., Sell S.A., Totterdell I.J. Acceleration of global warming due to carbon-cycle feedbacks in a coupled climate model. *Nature*, 404:184–187, 2000.

[9] Grass D. Numerical computation of the optimal vector field: Exemplified by a fishery model. *Journal of Economic Dynamics & Control*, 36:1626–1658, 2012.

[10] Grass D., Caulkins J.P., Feichtinger G., Tragler G., Behrens D.A. *Optimal Control of Nonlinear Processes – With Applications in Drugs, Corruption, and Terror*. Springer, Heidelberg, 2008.

[11] IPCC. *Climate change 2001: The Scientific Basis. Contribution of Working Group I to the Third Assessment Report of the Intergovernmental Panel on Climate Change*. Cambridge University Press, Cambridge, United Kingdom and New York, NY, USA, 2001.

[12] IPCC. *Climate Change 1995: Economic and Social Dimensions of Climate Change: Contribution of Working Group III to the Second Assessment Report of the Intergovernmental Panel on Climate Change*. Cambridge University Press, Cambridge, New York and Melbourne, 1996.

[13] Acemoglu D. *Introduction to Modern Economic Growth*. Princeton University Press, Princeton, 2009.

[14] UNFCCC. The Cancun Agreement: Outcome of the work of the Ad Hoc Working Group on Long-term Cooperative Action under the Convention. In *Report of the Conference of the Parties on its sixteenth session, held in Cancun from 29 November to 10 December 2010*, 2011.

List of Figures